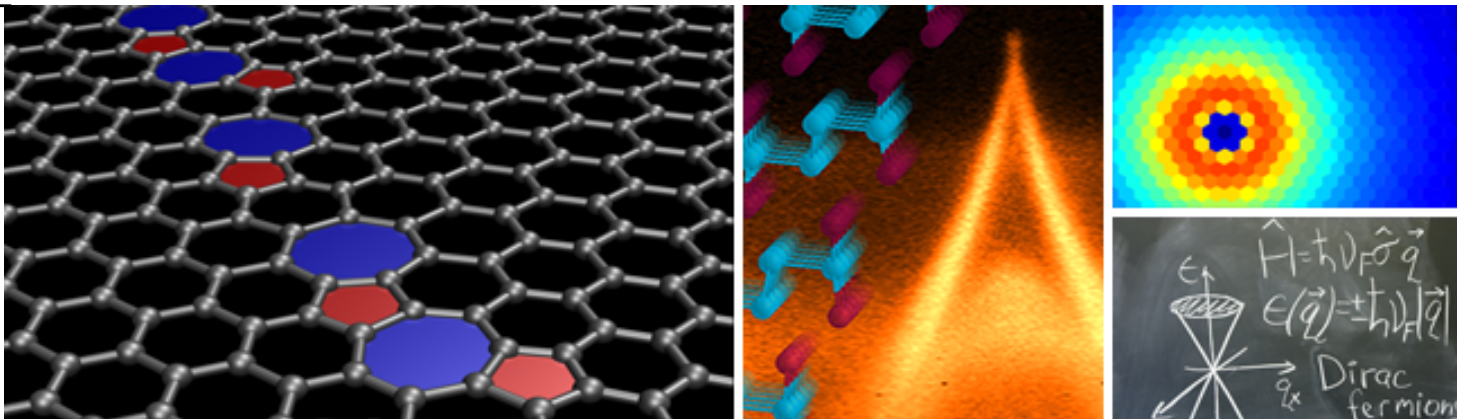


# Topological defects in graphene and other 2D materials



**Oleg Yazyev**

Institute of Physics  
Ecole Polytechnique Fédérale de Lausanne (EPFL)  
Switzerland



- Would graphene remain single crystalline at large length scales?

- Unlikely.

# Outline

- Topological defects in graphene
- Experimental evidence
- Buckling transition of grain boundaries in graphene
- Electronic transport phenomena
  - Electronic transport across periodic grain boundaries
  - Dislocations as resonant scattering sources
  - Valley filtering using periodic line defects in graphene
- Topological defects in MoS<sub>2</sub> and other dichalcogenides
- Spin-orbit gap, spin- and valley-filtering, etc.

## Further information

For review see:

nature  
nanotechnology

FOCUS | REVIEW ARTICLE

PUBLISHED ONLINE: 17 AUGUST 2014 | DOI: 10.1038/NNANO.2014.166

# Polycrystalline graphene and other two-dimensional materials

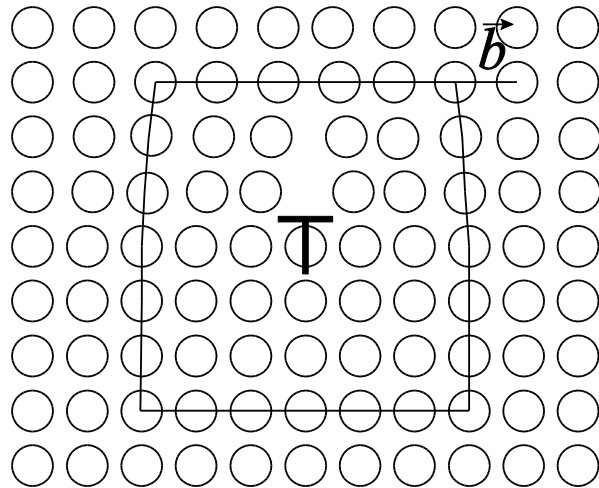
Oleg V. Yazyev<sup>1</sup> and Yong P. Chen<sup>2</sup>

**Graphene, a single atomic layer of graphitic carbon, has attracted intense attention because of its extraordinary properties that make it a suitable material for a wide range of technological applications. Large-area graphene films, which are necessary for industrial applications, are typically polycrystalline — that is, composed of single-crystalline grains of varying orientation joined by grain boundaries. Here, we present a review of the large body of research reported in the past few years on polycrystalline graphene. We discuss its growth and formation, the microscopic structure of grain boundaries and their relations to other types of topological defect such as dislocations. The Review further covers electronic transport, optical and mechanical properties pertaining to the characterizations of grain boundaries, and applications of polycrystalline graphene. We also discuss research, still in its infancy, performed on other two-dimensional materials such as transition metal dichalcogenides, and offer perspectives for future directions of research.**

O. V. Yazyev and Y. P. Chen, *Nature Nanotechnol.* **9**, 755 (2014)

# Topological defects

## Dislocation



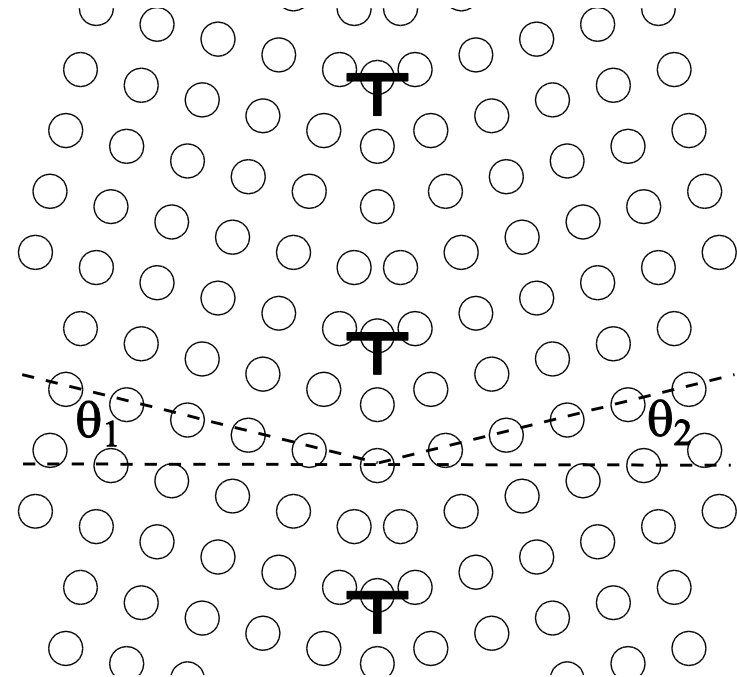
Topological invariant:

$\vec{b}$  - Burgers vector

In graphene:

In 2D only edge dislocations  
( $\vec{b} \perp \xi$ ) are possible

## Grain boundary



$\theta = \theta_1 + \theta_2$  - misorientation angle;

$\psi = |\theta_1 - \theta_2|$  - tilt angle

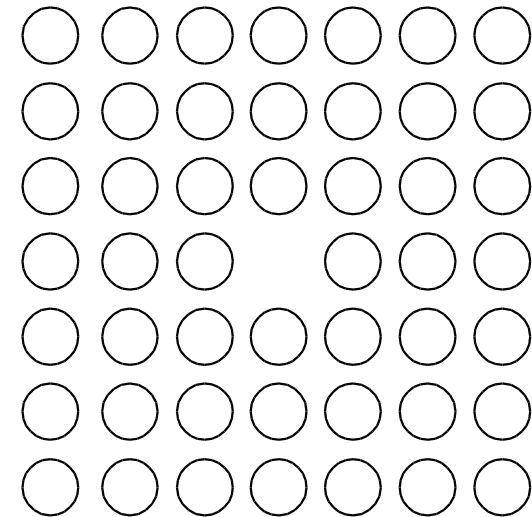
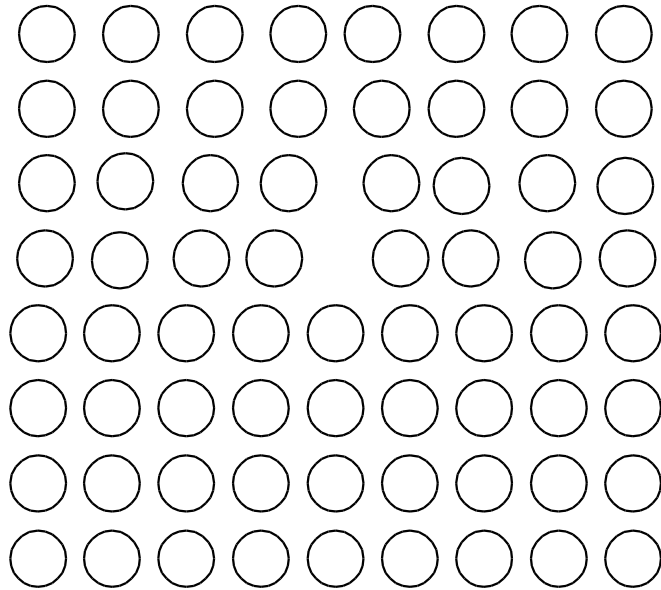
In 2D only tilt grain boundaries are possible. More specifically, in graphene  
 $\theta \in [0, 60^\circ], \psi \in [0, \theta]$

# Non-locality of topological disorder

**Dislocations**

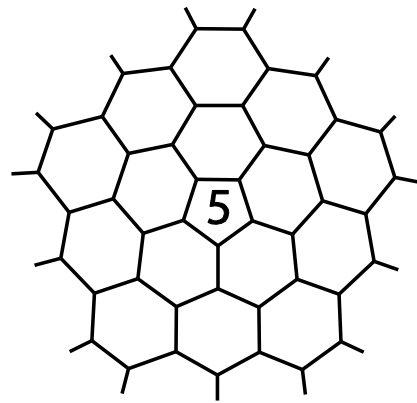
vs.

**point defects**

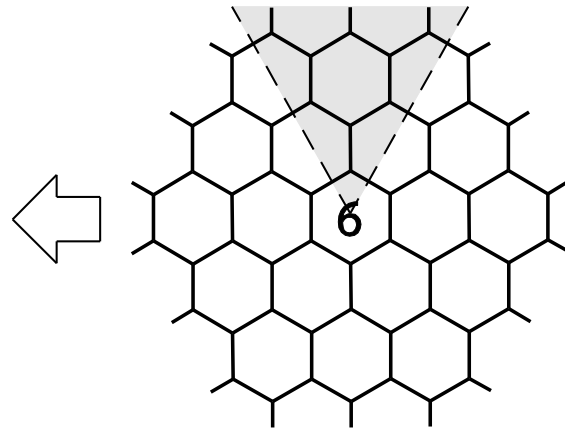


# Disclinations in graphene

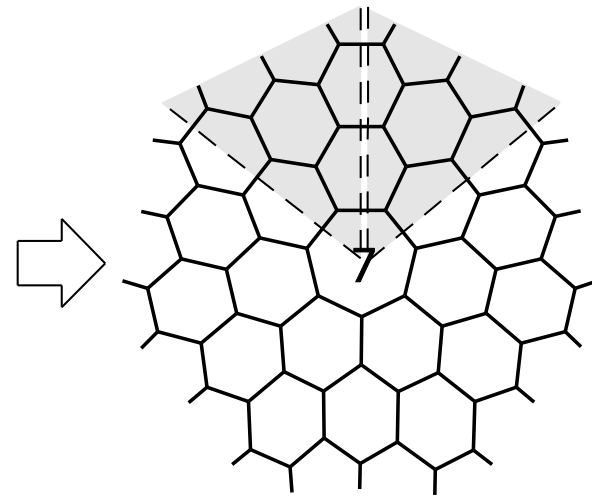
Volterra cut-and-glue construction



positive disclination  
 $s = 60^\circ$



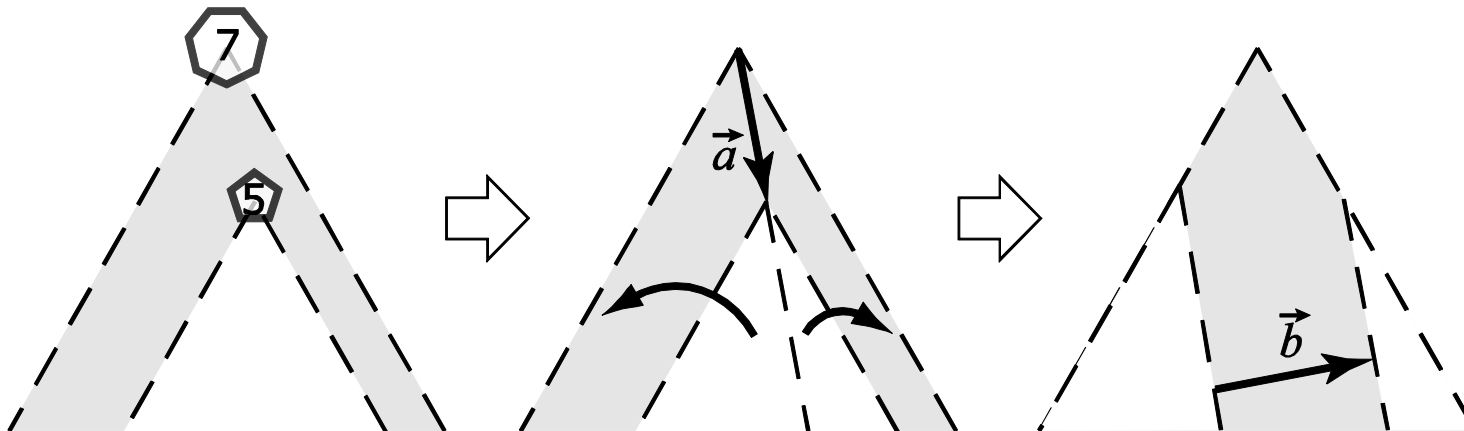
ideal graphene



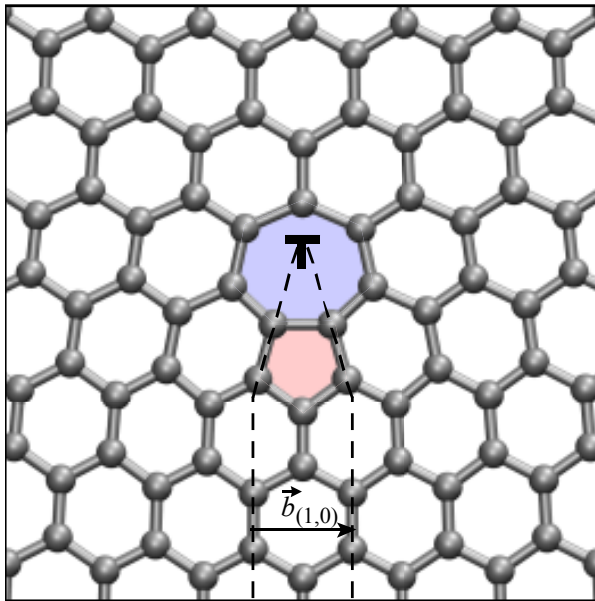
negative disclination  
 $s = -60^\circ$

Seung & Nelson, 1988

Dislocation = pair of disclinations

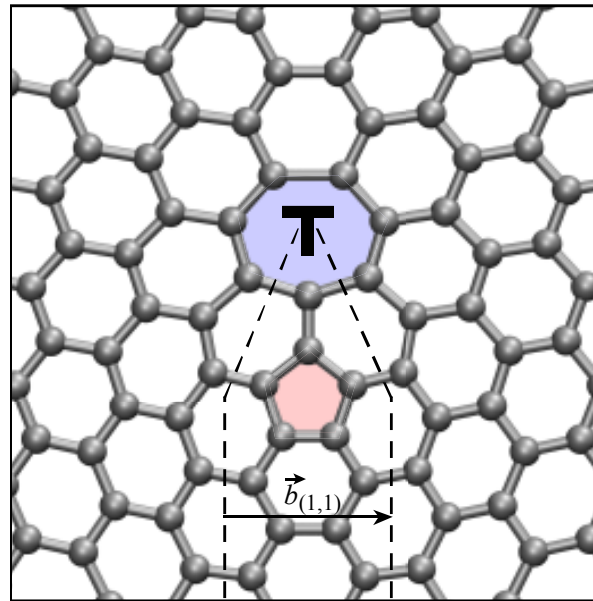


# Dislocations in graphene



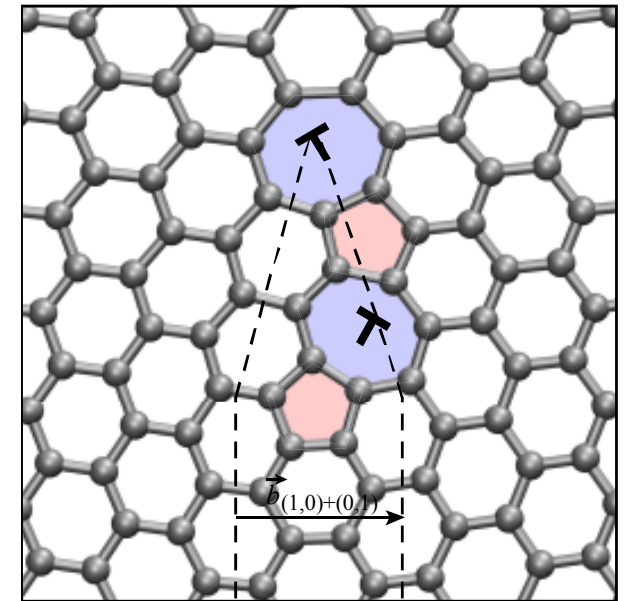
(1,0) dislocation

$$|\vec{b}| = \sqrt{3}d_{CC} = 2.46\text{\AA}$$



(1,1) dislocation

$$|\vec{b}| = 3d_{CC} = 4.23\text{\AA}$$



(1,0)+(0,1) dislocation

$$|\vec{b}| = 3d_{CC} = 4.23\text{\AA}$$



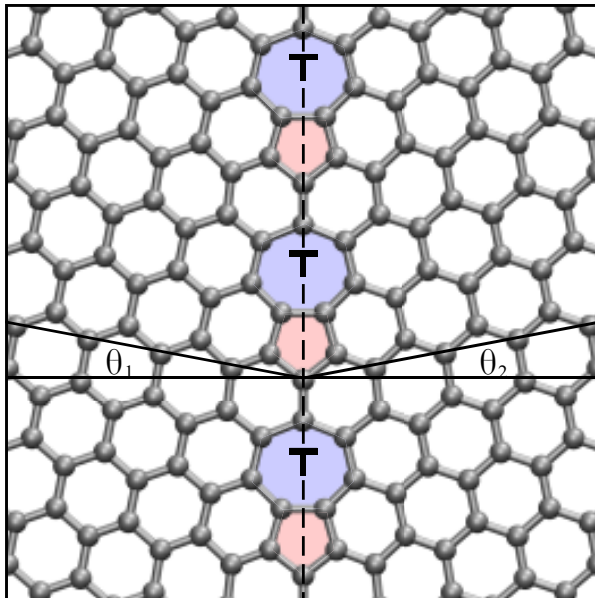
# Large-angle symmetric grain boundaries in graphene

Frank's equations:

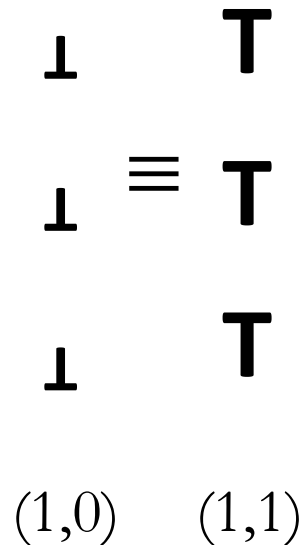
GB's along armchair direction:

$$\theta = 2 \arcsin \frac{|\vec{b}_{(1,0)}|}{2d_{(1,0)}}$$

$$0^\circ < \theta < 21.8^\circ$$



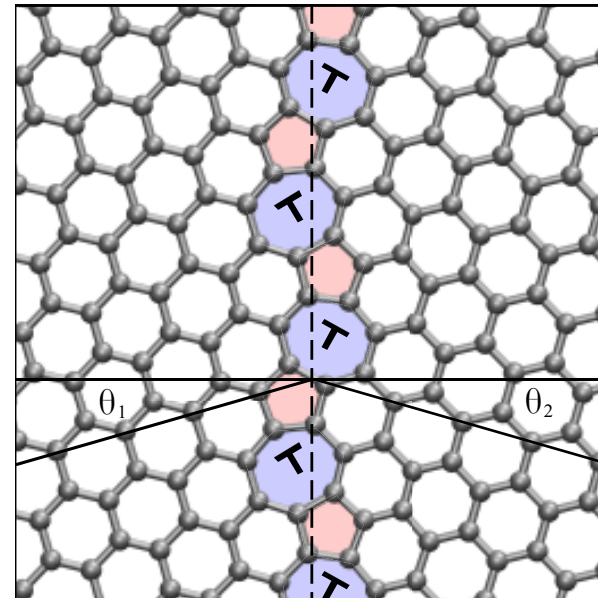
LAGB I  
 $\theta = 21.8^\circ$



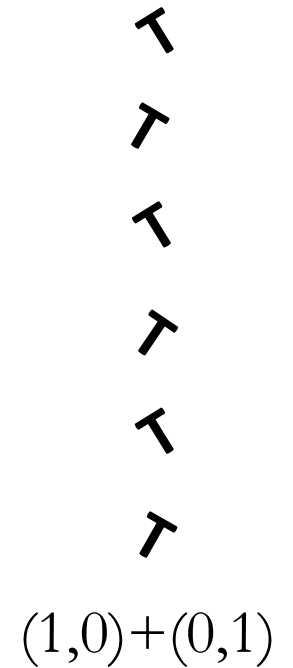
GB's along zigzag direction:

$$\theta = 60^\circ - 2 \arcsin \frac{|\vec{b}_{(1,1)}|}{2d_{(1,1)}}$$

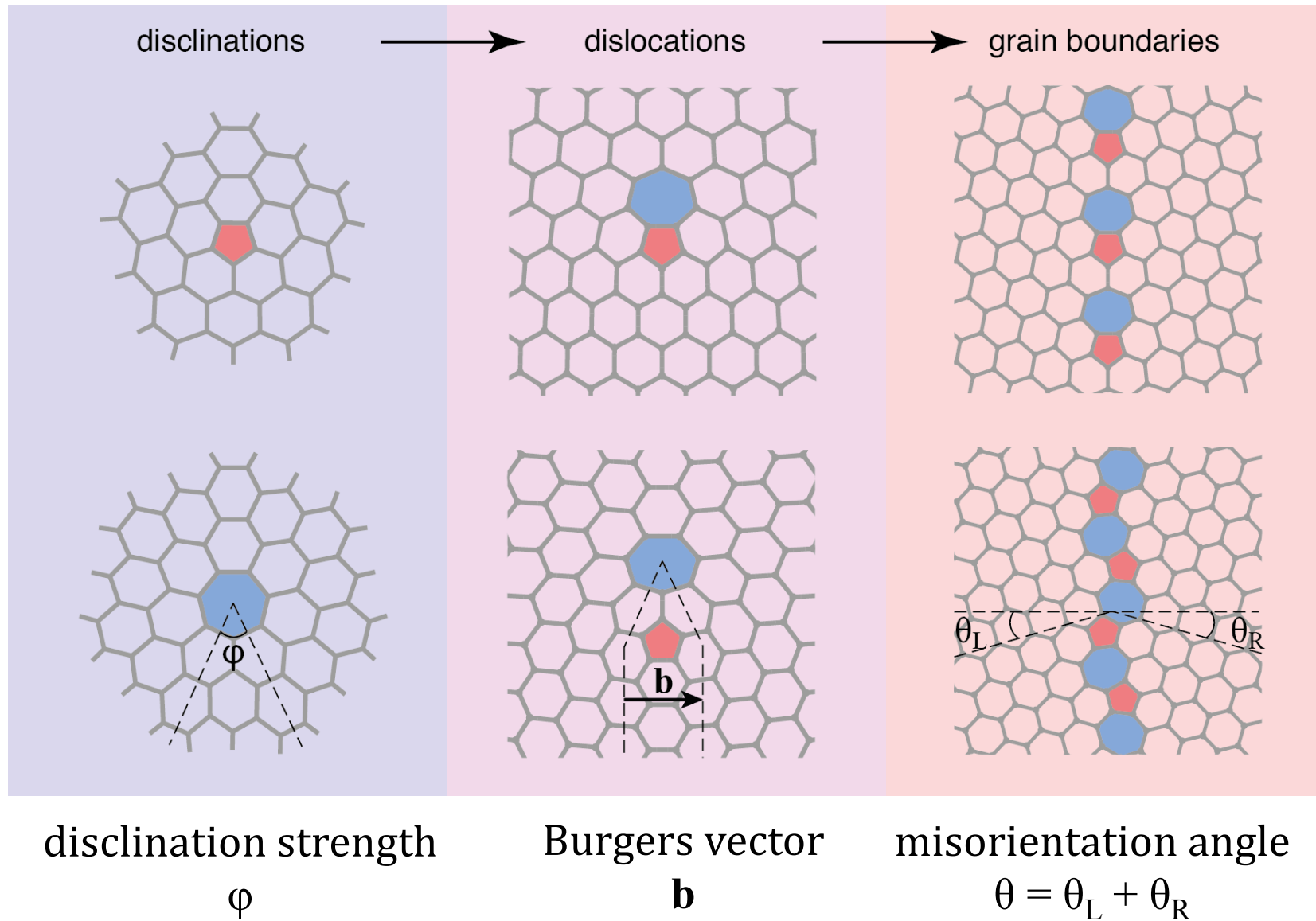
$$21.8^\circ < \theta < 60^\circ$$



LAGB II  
 $\theta = 32.2^\circ$



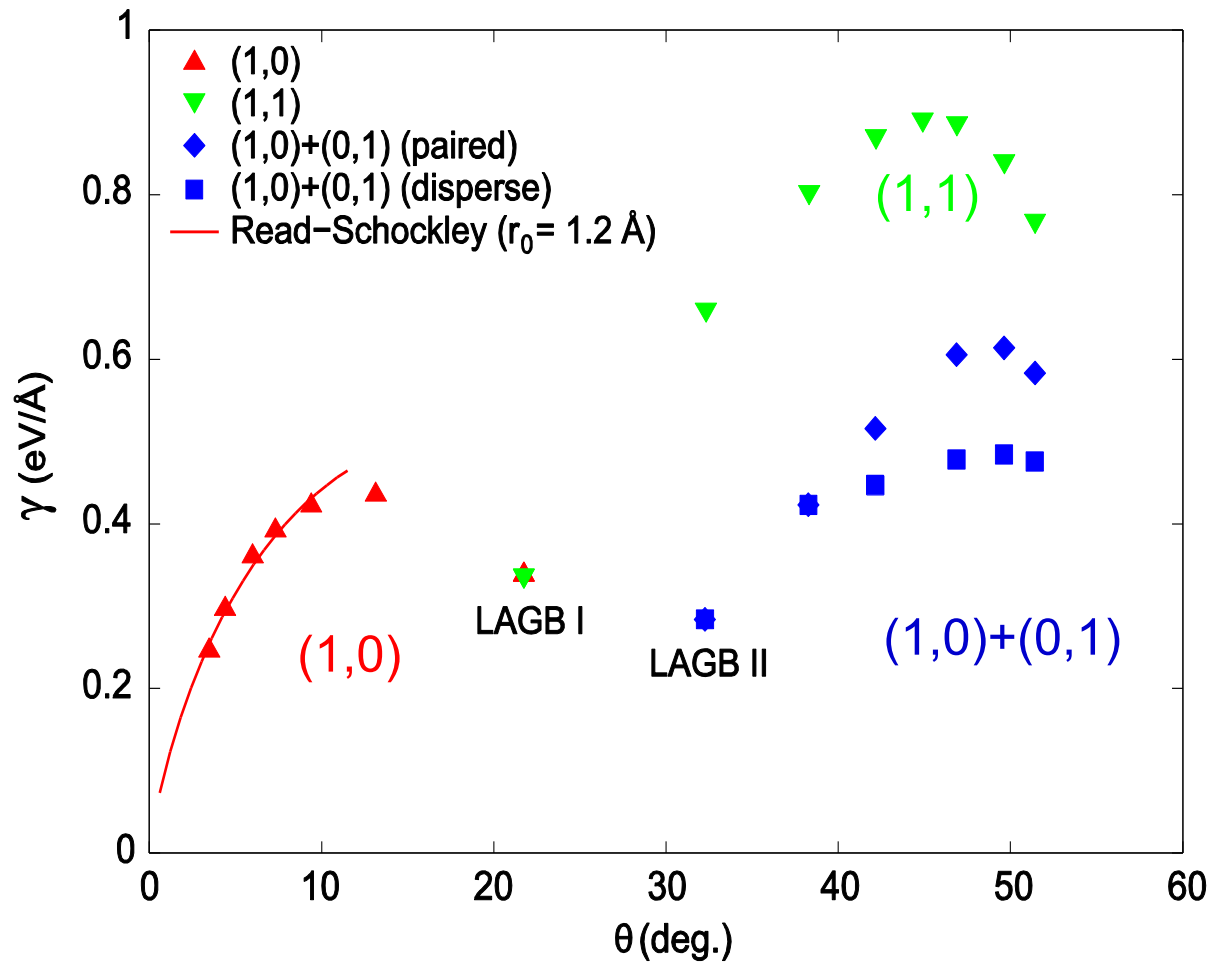
# Polycrystalline graphene and topological defects



Yazyev & Louie, Phys. Rev. B **81**, 195420 (2010); also results by group of Yakobson

# Grain boundary energetics (flat)

DFT-GGA results



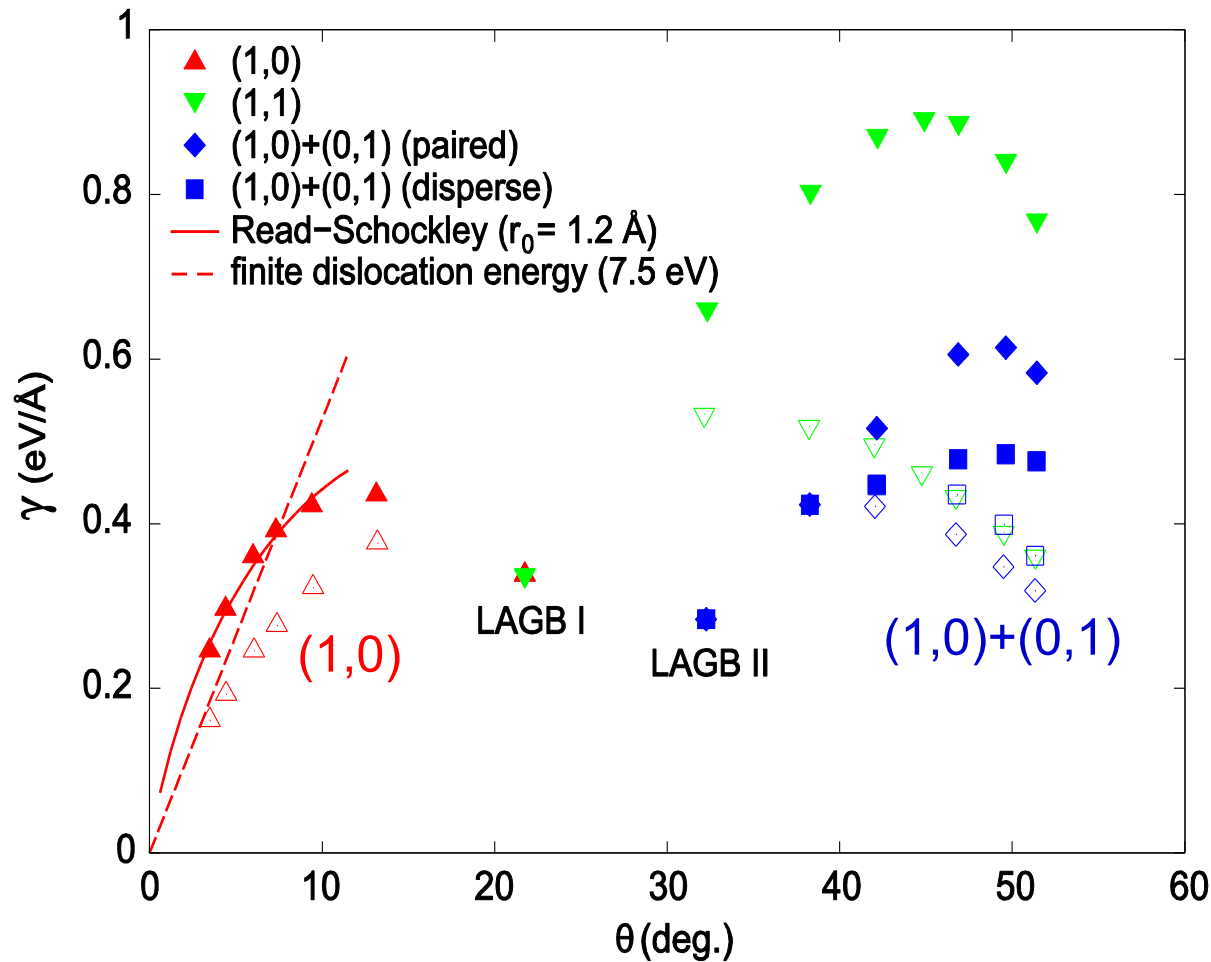
Flat regime (bulk-like):  
Read-Shockley equation

$$\gamma(\theta) = \frac{\mu |\vec{b}|}{4\pi(1-\nu)} \theta (A - \ln \theta)$$

$$A = 1 + \ln\left(\frac{|\vec{b}|}{2\pi r_0}\right) \quad r_0 = 1.2 \text{ \AA}$$

# Grain boundary energetics (buckled)

DFT-GGA results



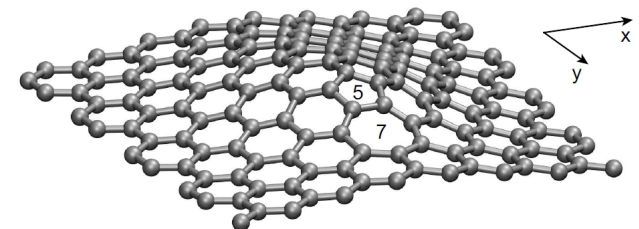
Flat regime (bulk-like):  
Read-Shockley equation

$$\gamma(\theta) = \frac{\mu |\vec{b}|}{4\pi(1-\nu)} \theta (A - \ln \theta)$$

$$A = 1 + \ln\left(\frac{|\vec{b}|}{2\pi r_0}\right) \quad r_0 = 1.2 \text{ \AA}$$

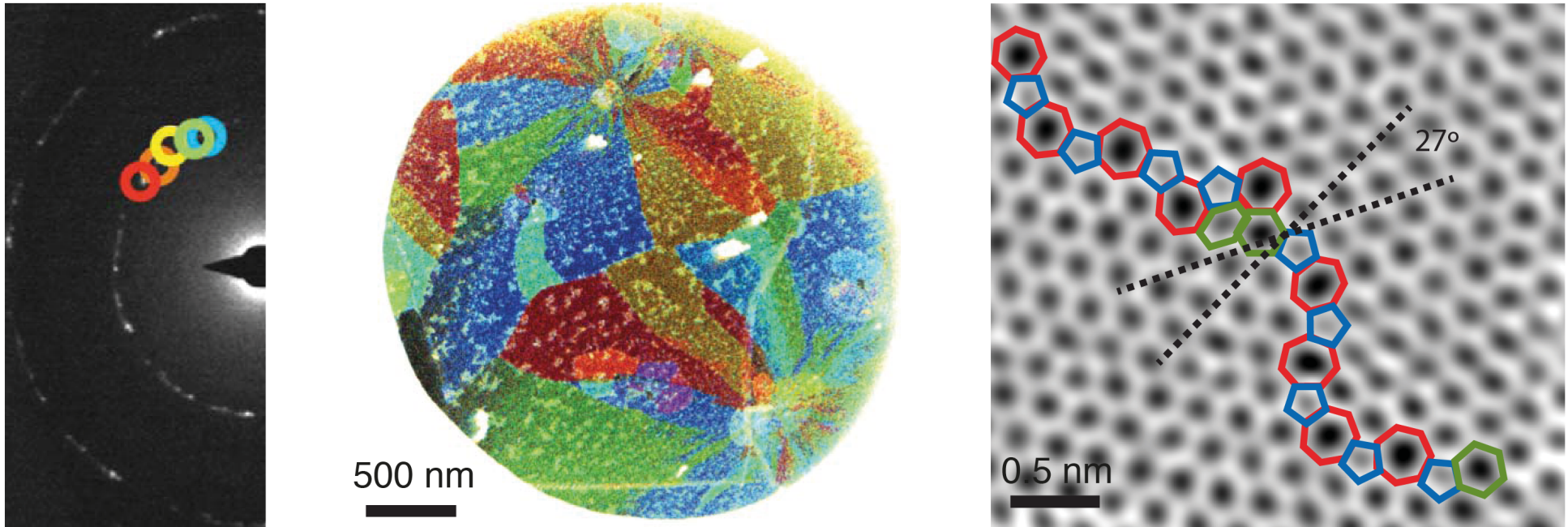
Buckled regime (membrane)  
Finite dislocation energy

$$\gamma(\theta) = \frac{E_f \theta}{|\vec{b}|} \quad E_f = 7.5 \text{ eV}$$



# Experimental evidence

Epitaxial graphene grown on Cu substrates

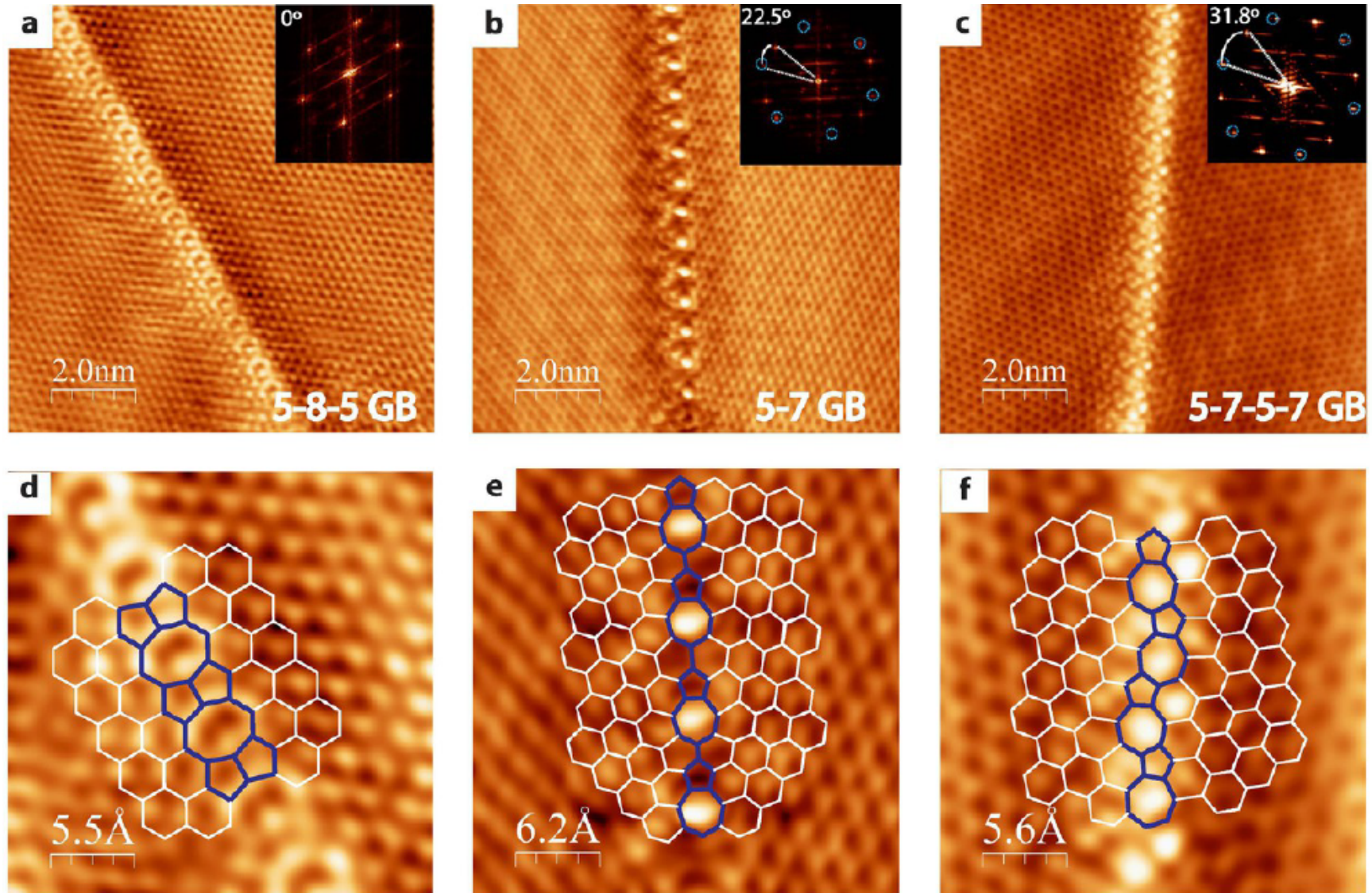


Reproduced from Huang *et al.*, Nature **469**, 389 (2011).

Almost simultaneously reported in  
Kim *et al.*, ACS Nano **5**, 2142 (2011),  
An *et al.*, ACS Nano **5**, 2433 (2011),  
followed by many others.

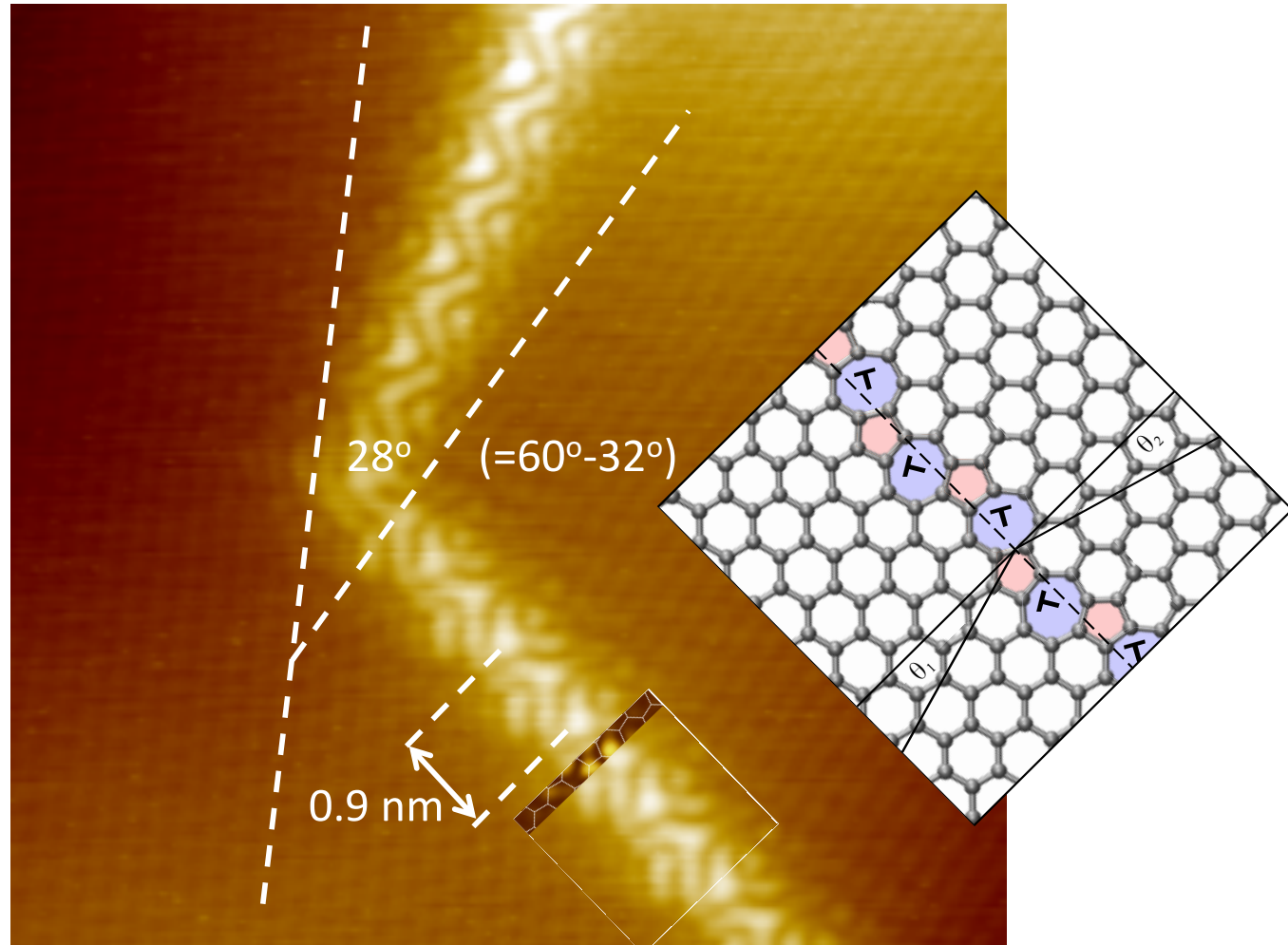
# Ordered GBs in graphene

Annealed CVD graphene



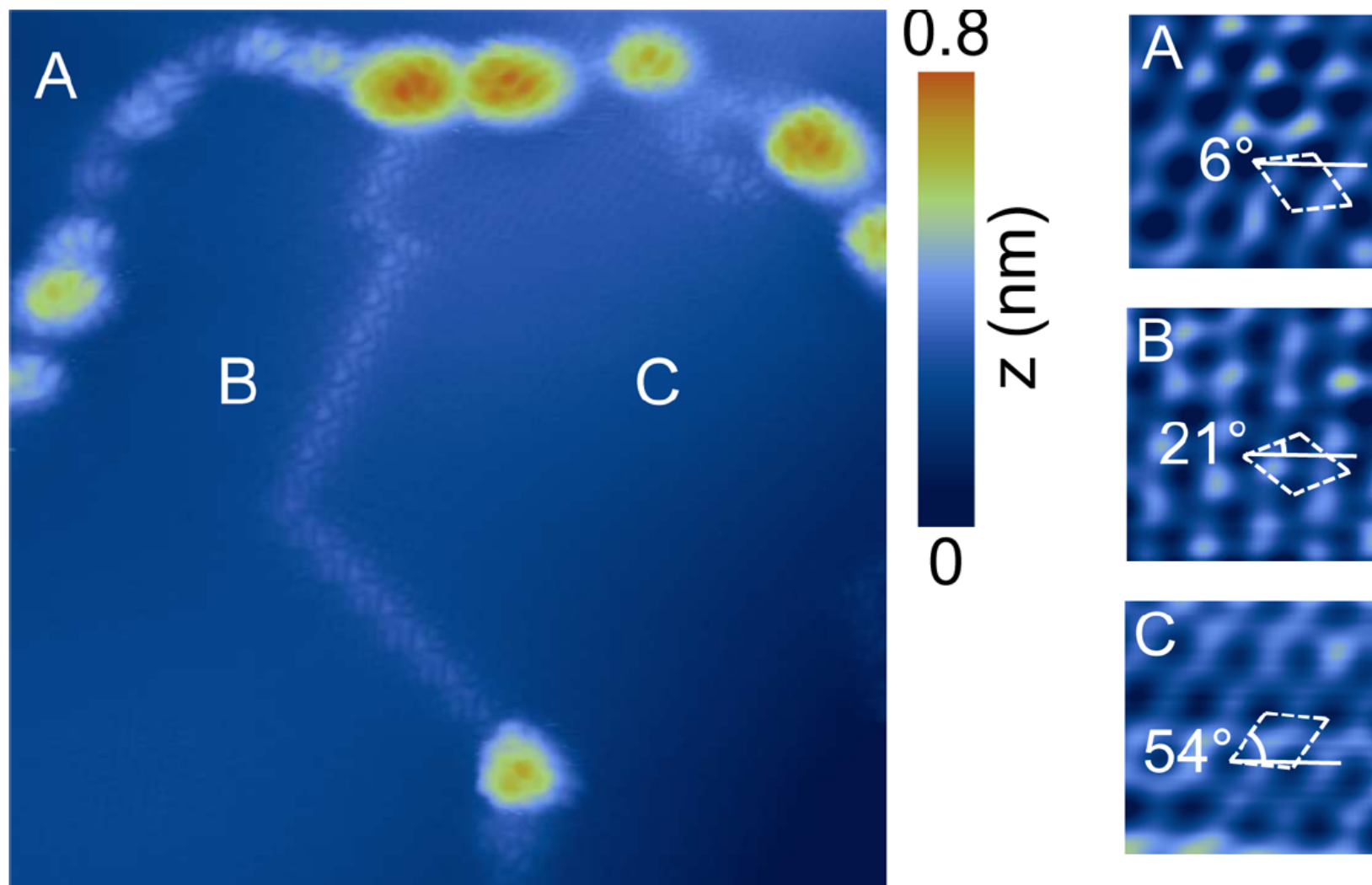
# Experimental evidence

Large-angle GB in epitaxial graphene on SiC(000-1).



Experiments: Vincent Repain (Paris VII); theory: Yazyev group (EPFL)

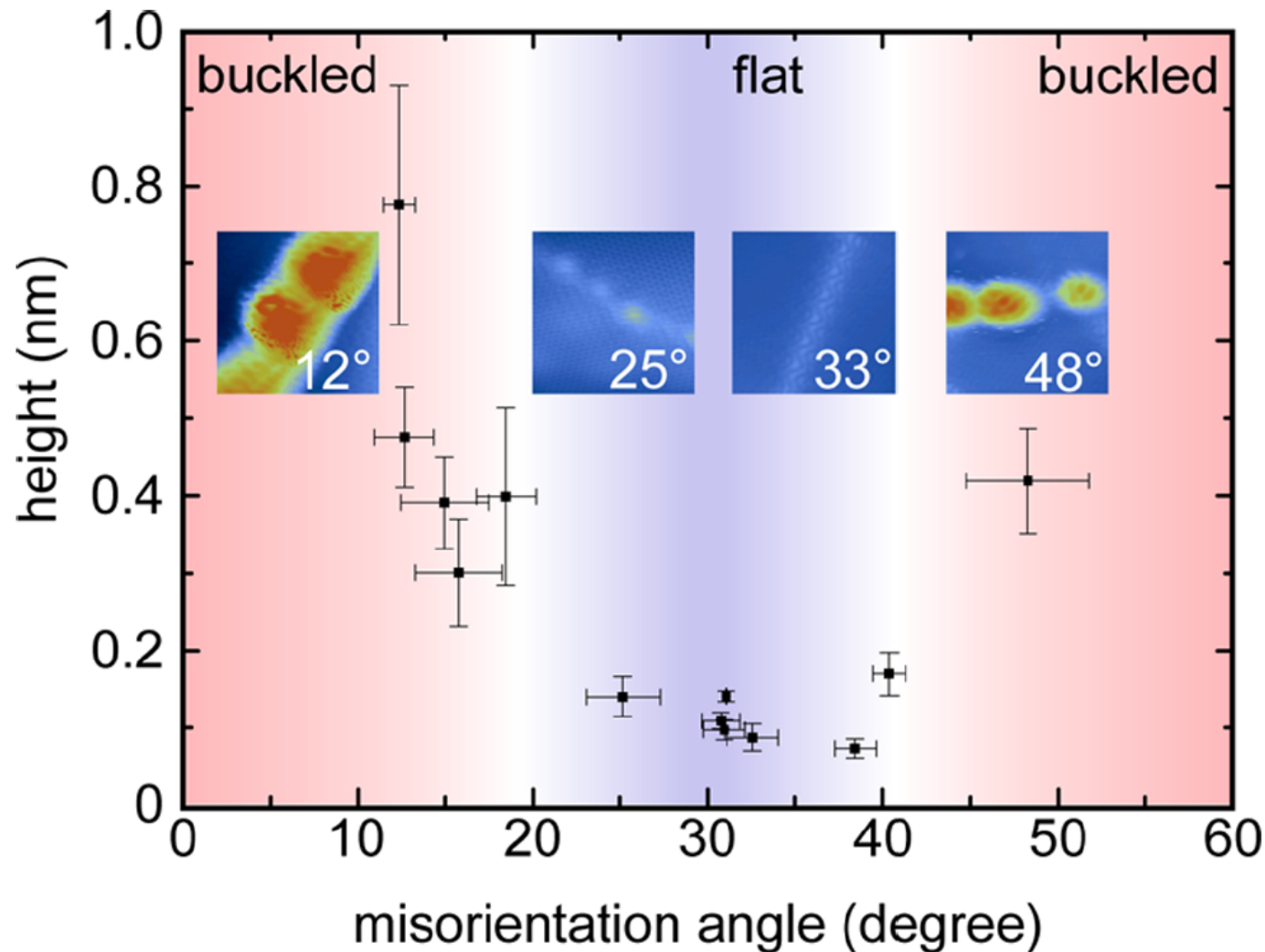
# Buckling transition of GBs in graphene





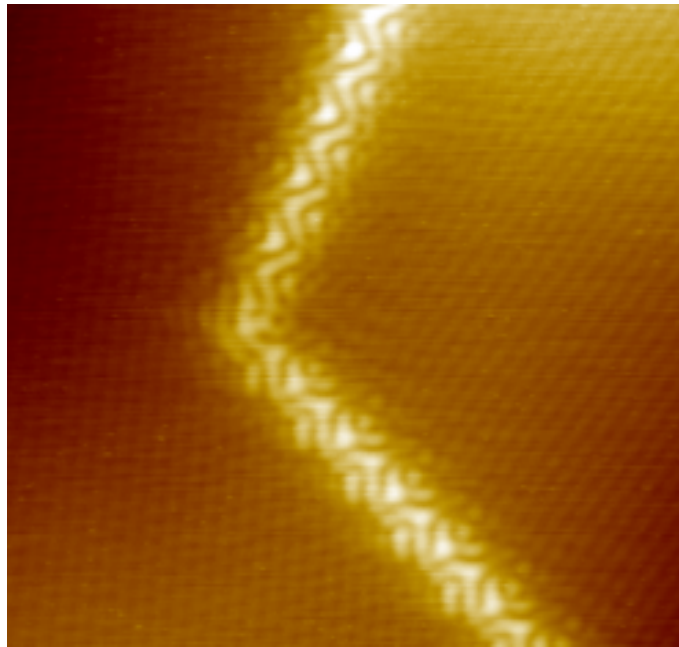
# Buckling transition of GBs in graphene

Buckling transition  $\theta_c = 19^\circ \pm 1^\circ$  (and symmetrically  $\theta_c = 41^\circ \pm 1^\circ$ )

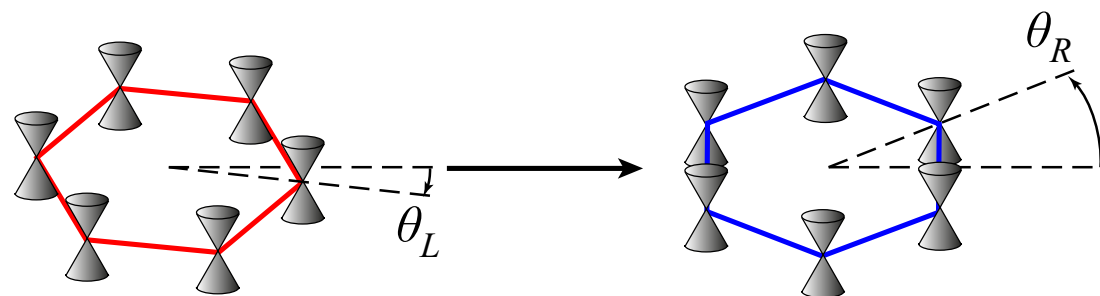
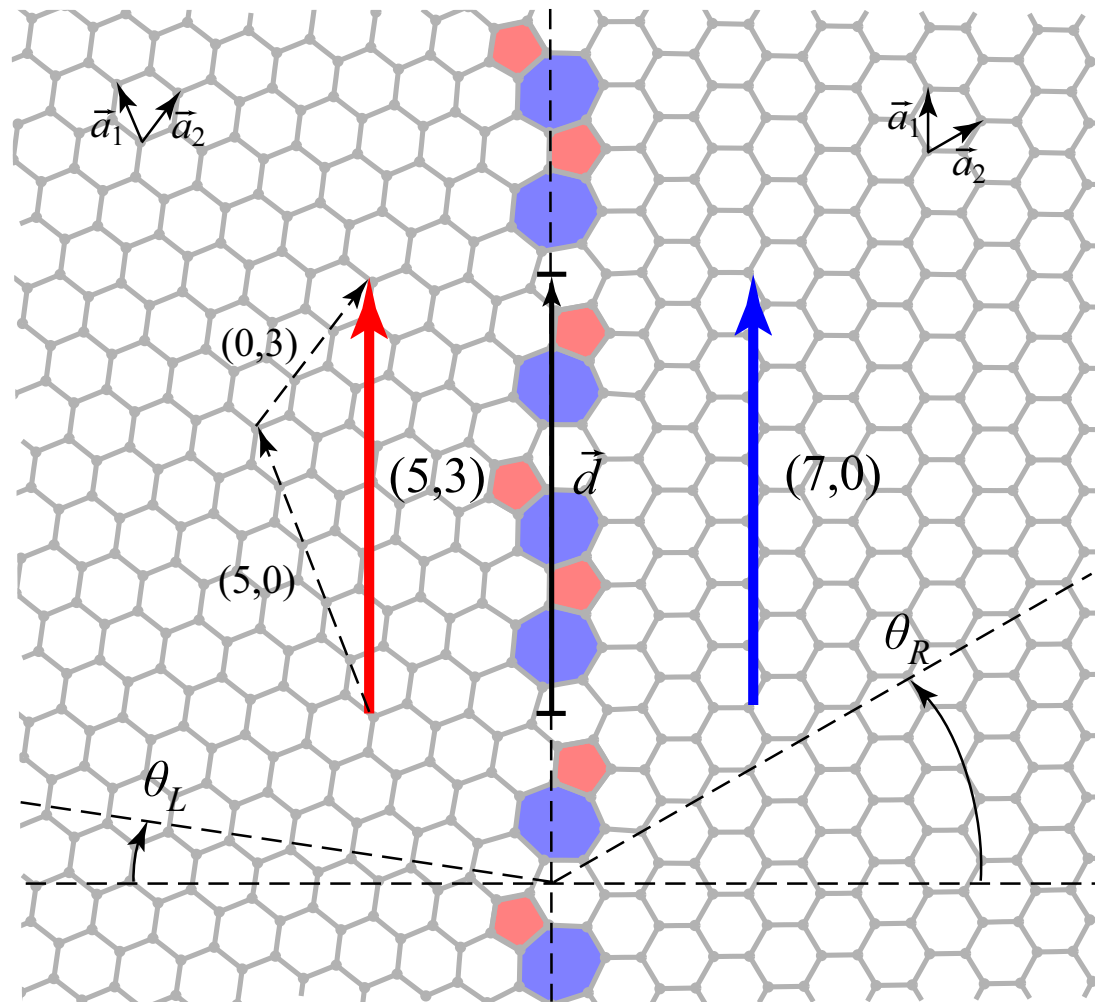


# I. Transport across periodic grain boundaries in graphene:

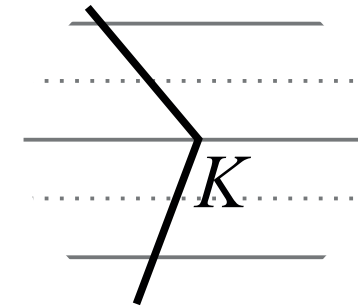
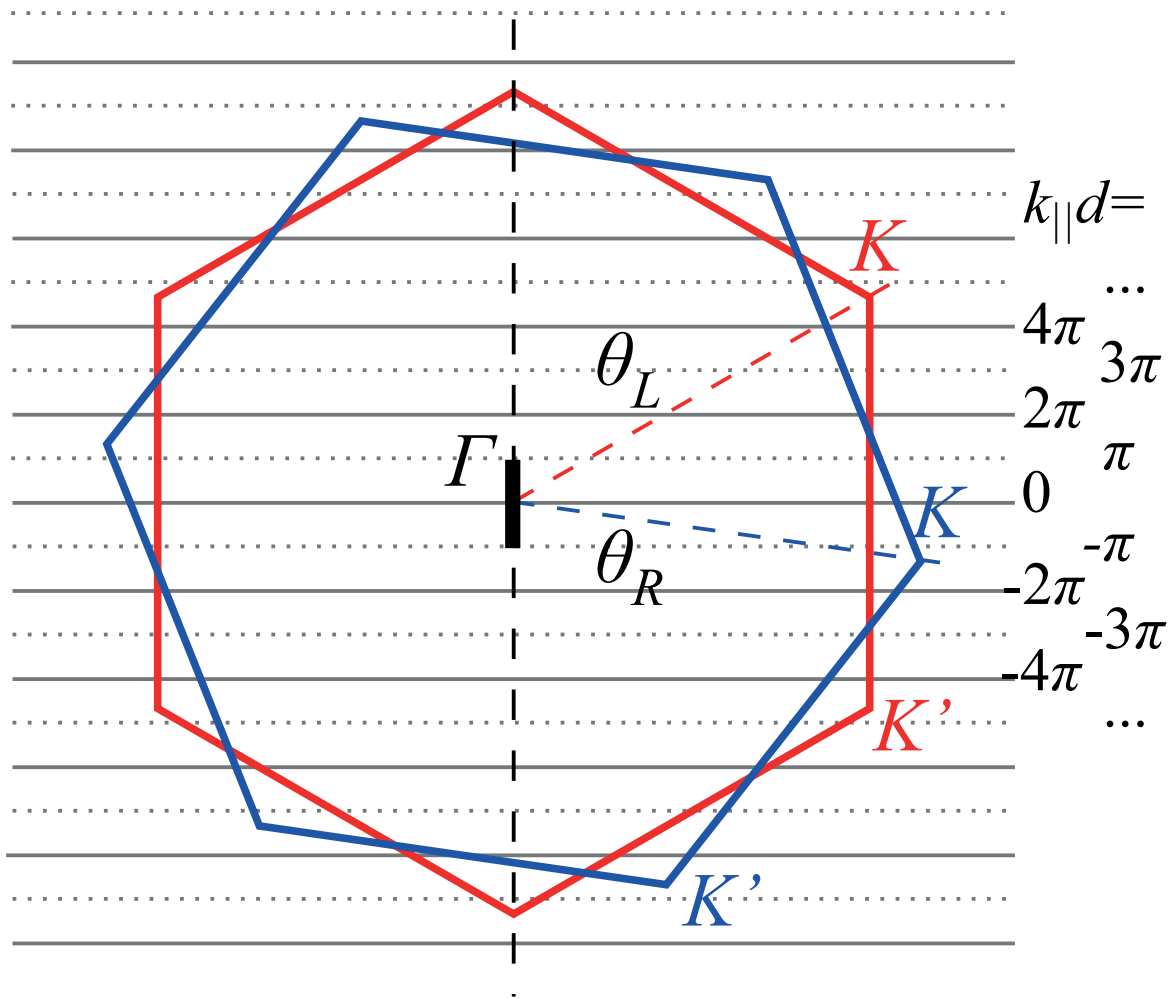
## Momentum conservation



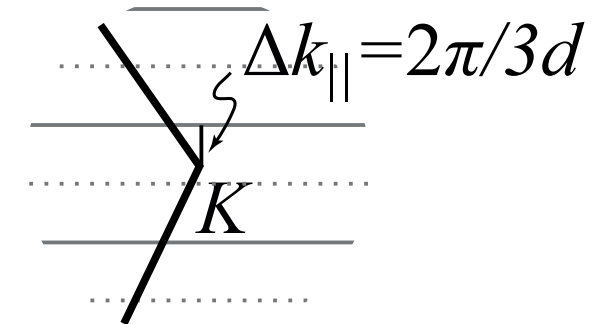
# Electronic transport in polycrystalline graphene



# Zone-folding approach

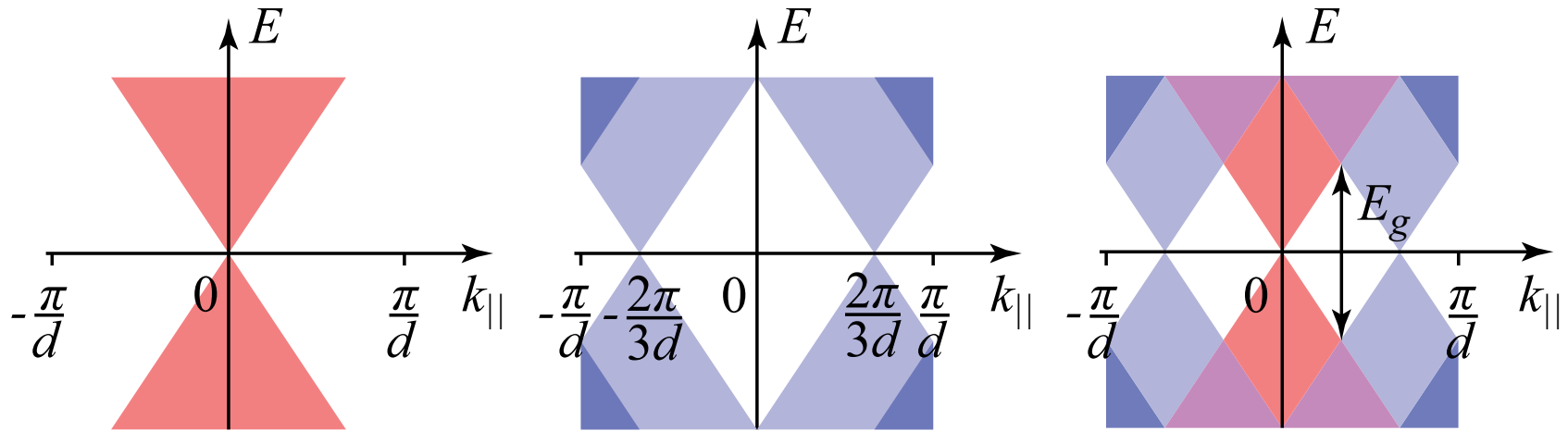


$$n - m = 3q$$



$$n - m \neq 3q$$

# Two distinct transport behaviors of periodic GBs



Transmission allowed:

■ Ia

■ Ib

■ II

$$\begin{aligned} n_L - m_L &= 3q \\ n_R - m_R &= 3q \end{aligned}$$

$$\begin{aligned} n_L - m_L &\neq 3q \\ n_R - m_R &\neq 3q \end{aligned}$$

$$\begin{aligned} n_L - m_L &= 3q & \text{or} & & n_L - m_L &\neq 3q \\ n_R - m_R &\neq 3q & & & n_R - m_R &= 3q \end{aligned}$$

Transport gap:

$$E_g = 0$$

$$E_g = 0$$

$$\begin{aligned} E_g &= \hbar v_F \frac{2\pi}{3d} \\ &\approx \frac{1.38}{d[\text{nm}]} [\text{eV}] \end{aligned}$$

# Non-equilibrium Green's function results (ballistic regime)

Transmission:

$$T = \text{Tr}(\Gamma_L G_S^\dagger \Gamma_R G_S)$$

Green's function (scatt. region):

$$G_S = (E^+ I - H_S - \Sigma_L - \Sigma_R)^{-1}$$

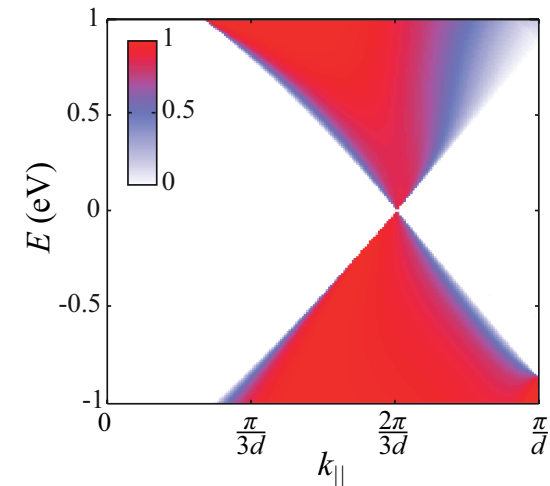
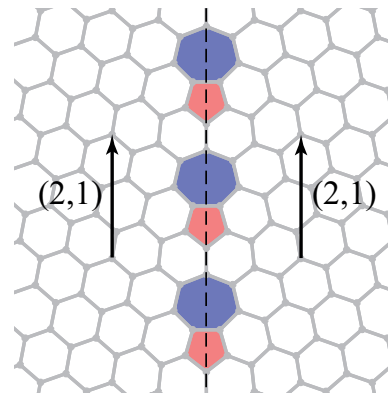
Coupling matrices (contacts):

$$\Gamma_{L(R)} = i(\Sigma_{L(R)} - \Sigma_{L(R)}^\dagger)$$

Class I (2,1)|(2,1)

$\Theta = 21.8^\circ$  (symmetric)

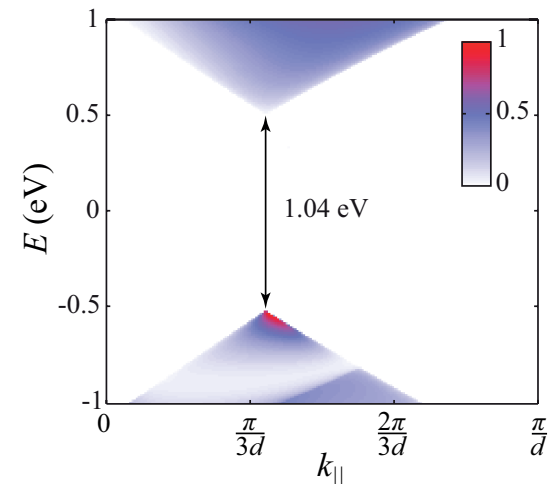
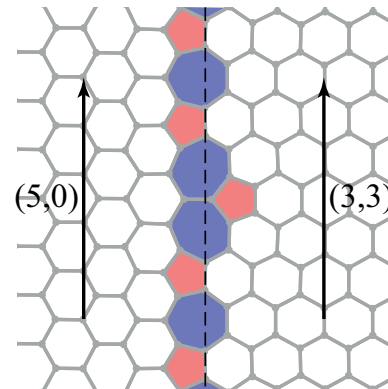
- highly transparent
- valleys separated in  $k_{||}$



Class II (5,0)|(3,3)

$\Theta = 30.0^\circ$  (asymmetric)

- large transport gap (1 eV)
- asymmetric, with misfit



# Non-equilibrium Green's function results (ballistic regime)

Transmission:

$$T = \text{Tr}(\Gamma_L G_S^\dagger \Gamma_R G_S)$$

Green's function (scatt. region):

$$G_S = (E^+ I - H_S - \Sigma_L - \Sigma_R)^{-1}$$

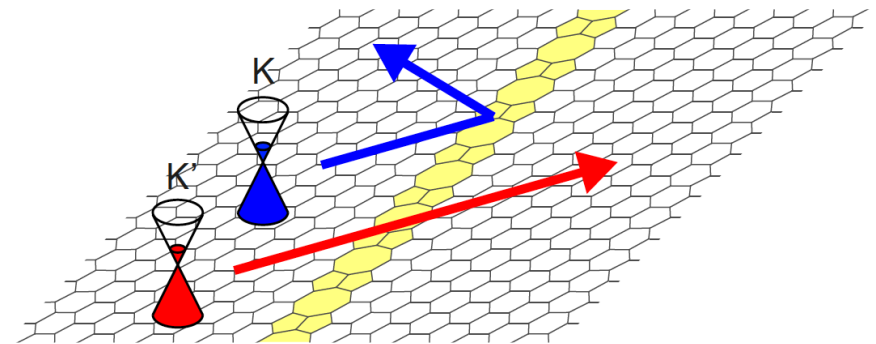
Coupling matrices (contacts):

$$\Gamma_{L(R)} = i(\Sigma_{L(R)} - \Sigma_{L(R)}^\dagger)$$

Class I (2,1)|(2,1)

$\Theta = 21.8^\circ$  (symmetric)

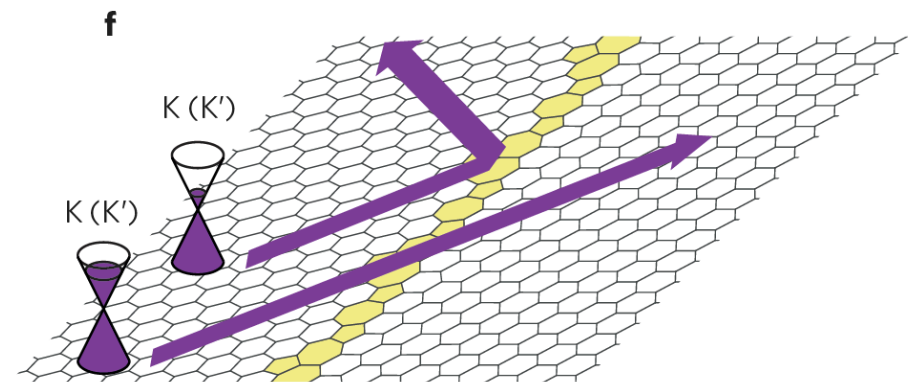
- highly transparent
- valleys separated in  $k_{\parallel}$  (valley filtering)



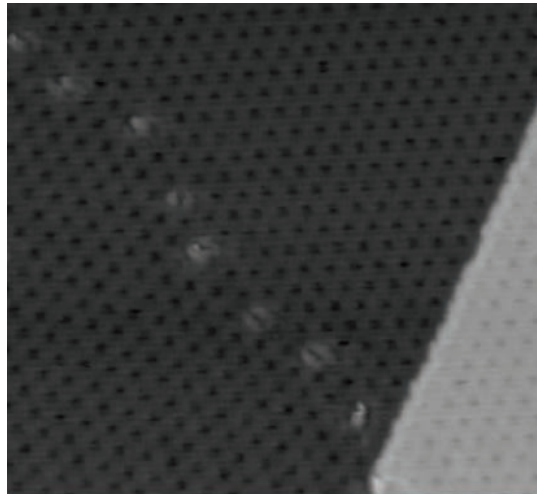
Class II (5,0)|(3,3)

$\Theta = 30.0^\circ$  (asymmetric)

- large transport gap (1 eV)
- asymmetric, with misfit

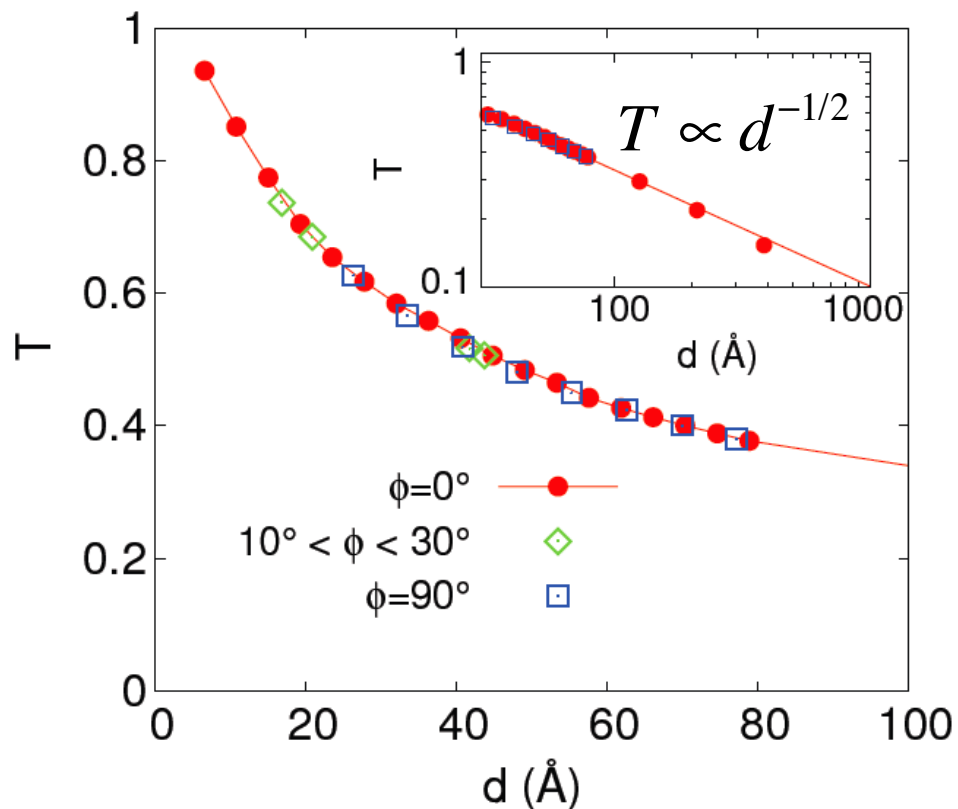
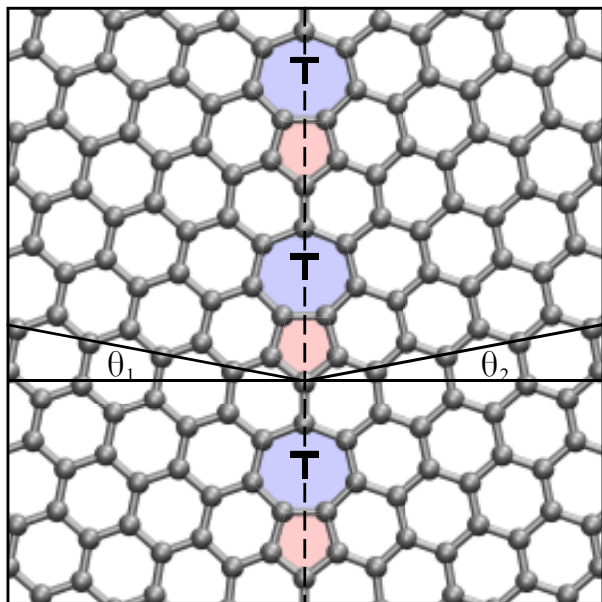


## II. Dislocations as resonant scattering centers





# Transport anomaly at low energies

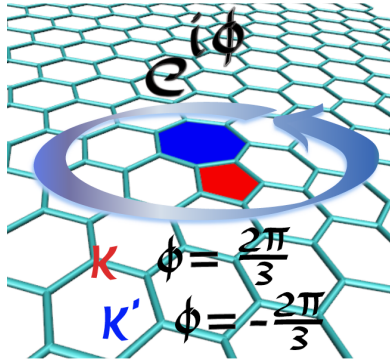


Transmission at  $E = 0$  decreases (!) as separation between dislocations increases.

Dislocations cannot be described in terms of scattering cross-sections, topological aspects are important

# Topological aspects in electronic transport

## Gauge field associated with dislocations



$$\varphi = \oint \mathbf{A} d\mathbf{r} = \mathbf{k} \cdot \mathbf{b}$$

Iordanskii & Koshchelev, Sov. Phys. JETP **63**, 820 (1986)

$\mathbf{b} = (1,0)$  dislocations (or any  $n - m \neq 3q$ ) are non-trivial ( $\mathbf{k} \cdot \mathbf{b} = \frac{2\pi}{3}$ )  
 $\mathbf{b} = (1,1)$  dislocations (or any  $n - m = 3q$ ) are trivial ( $\mathbf{k} \cdot \mathbf{b} = 0$ )

Analogy with Aharonov-Bohm effect (for the 1<sup>st</sup> case)

$$\Phi = 1/3 \Phi_0 \text{ } (-1/3 \Phi_0) \text{ for } \tau = +1 \text{ } (\tau = -1)$$

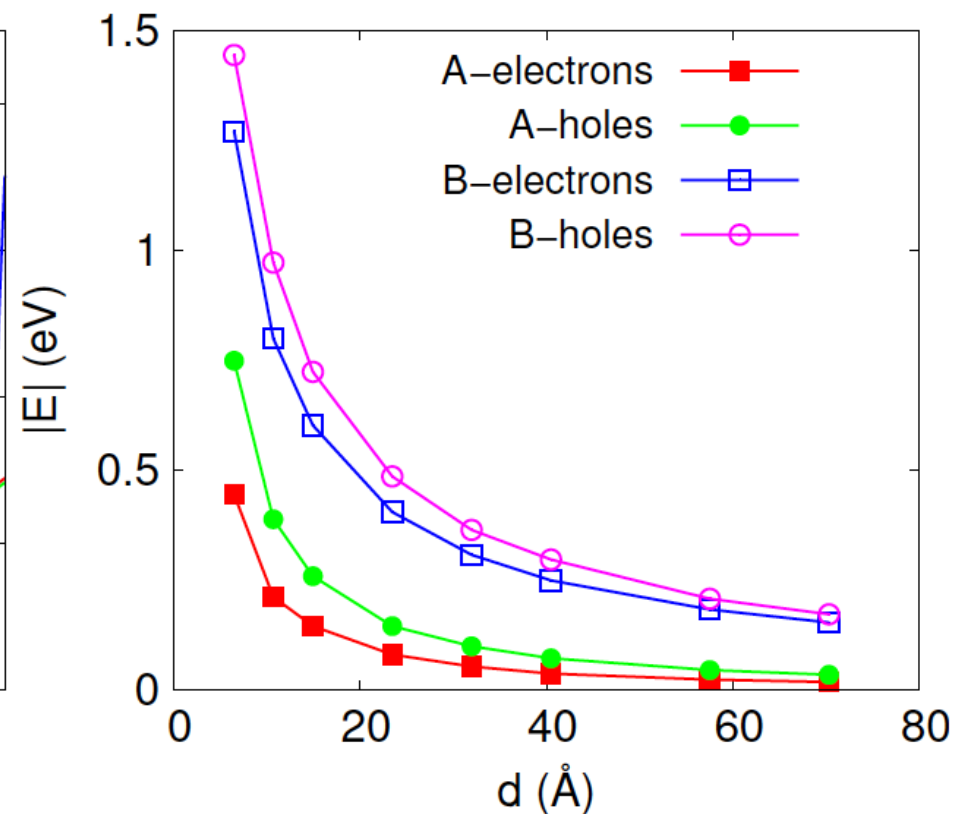
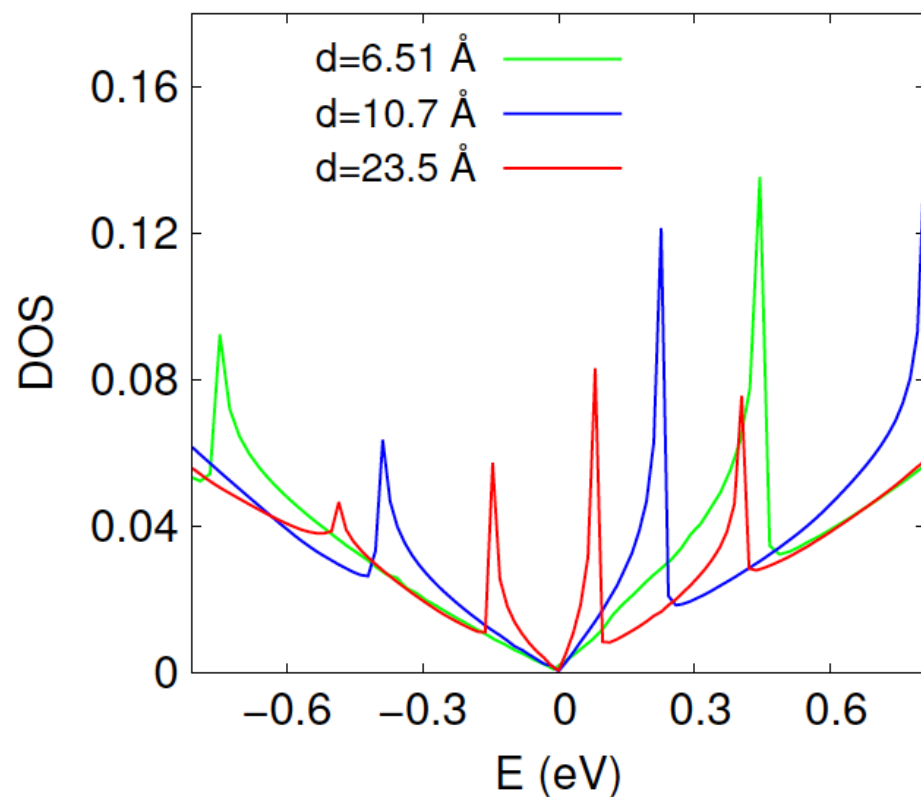
Give rise to zero-energy modes

$$LDOS(r, E) \propto r^{-4/3} |E|^{-1/3}$$

Mesaros *et al.*, PRB **82**, 205119 (2010)

# Hybridization of zero-modes

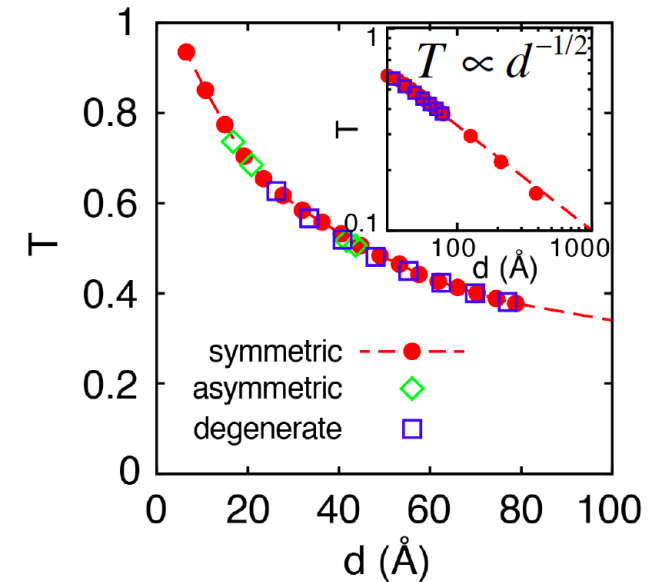
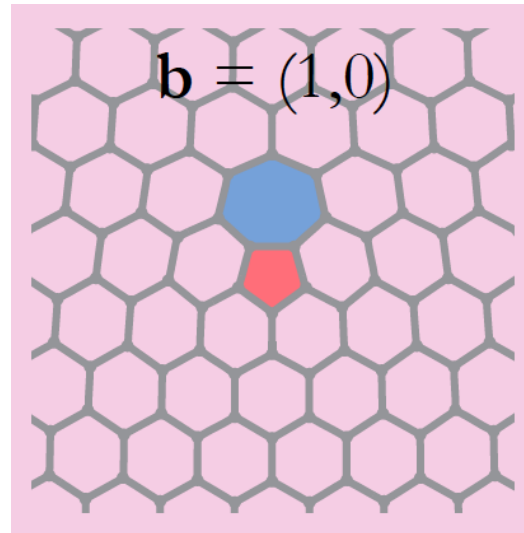
Resonant backscattering on zero-energy states



# Topological aspects: numerical results

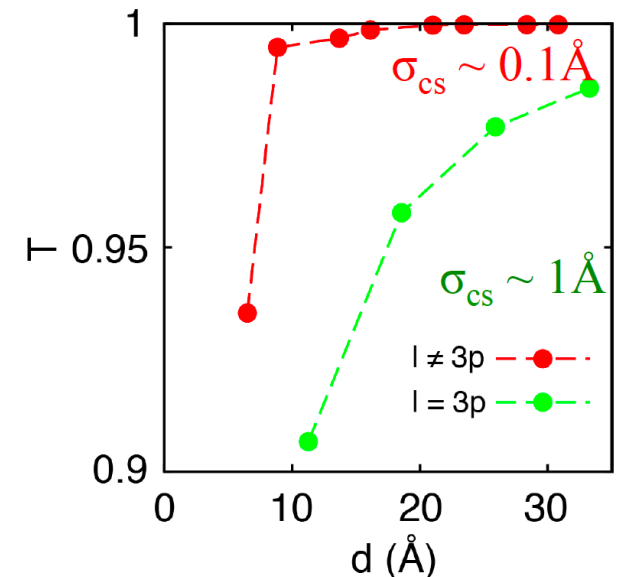
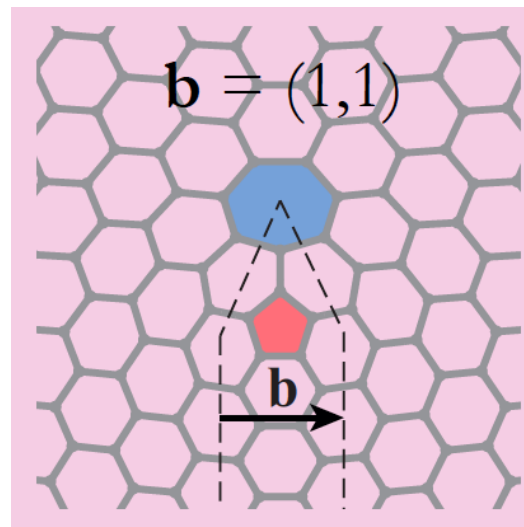
$\mathbf{b} = (1,0)$  dislocations:

- resonant scattering sources at  $E = 0$
- anomalous dependence of conductance on dislocation density

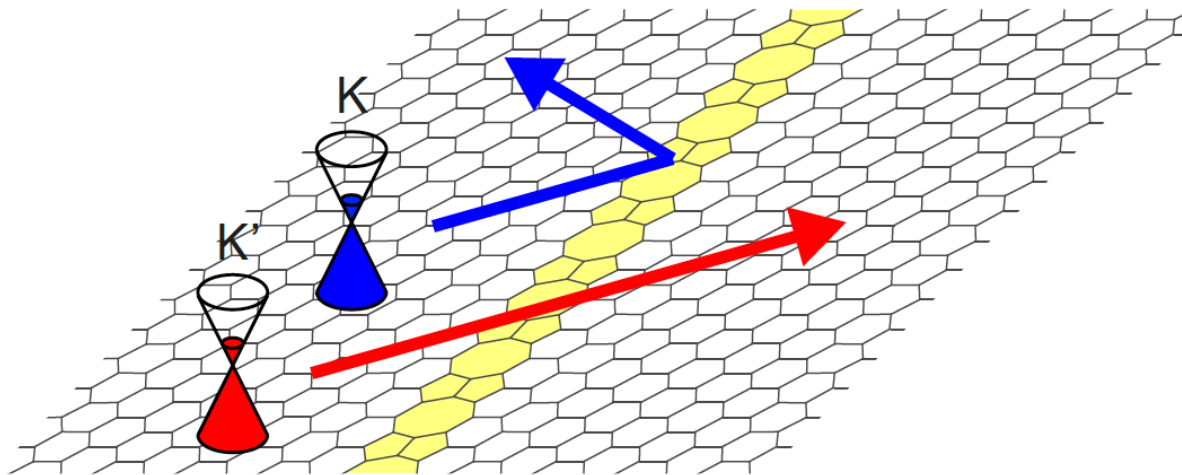


$\mathbf{b} = (1,1)$  dislocations:

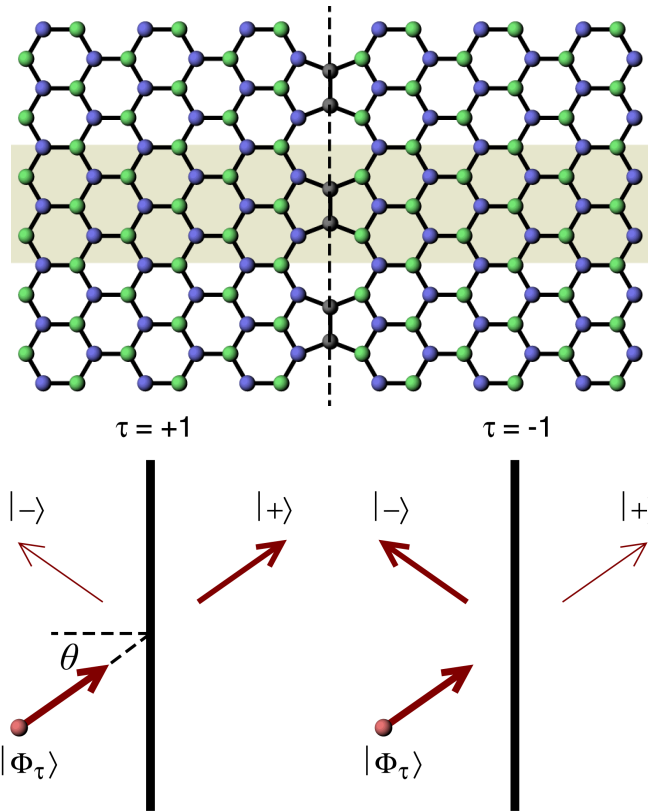
- small scattering cross-sections
- behave like point defects (topologically trivial)



### III. Valley filtering with line defects



# Valley filtering with 5-5-8 line defect



Gunlycke & White, PRL **106**, 136806 (2011)

Eigenstates in graphene:

$$|\Phi_\tau\rangle = \frac{1}{\sqrt{2}}(|A\rangle + ie^{-i\theta}|B\rangle)$$

In the symmetry-adapted basis:

$$|\Phi_\tau\rangle = \frac{1+ie^{-i\theta}}{2}|+\rangle + \frac{1-ie^{-i\theta}}{2}|-\rangle$$

where

$$|\pm\rangle = \frac{1}{\sqrt{2}}(|A\rangle \pm |B\rangle)$$

Transmission:

$$T_\tau = |\langle +|\Phi_\tau\rangle|^2 = \frac{1}{2}(1 + \tau \sin\theta)$$

Valley polarization

$$P_\tau = \frac{T_\tau - T_{-\tau}}{T_\tau + T_{-\tau}} = \tau \sin\theta$$

In general, all periodic defects with  $k_{||}(K) \neq k_{||}(K')$  (e.g. class-Ib GBs) are expected to show valley filtering, because

$$T_\tau(\theta) = T(k_{||}) = T(-k_{||}) = T_{-\tau}(-\theta) \neq T_{-\tau}(\theta)$$

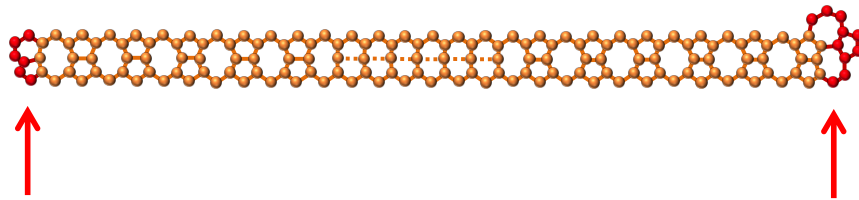
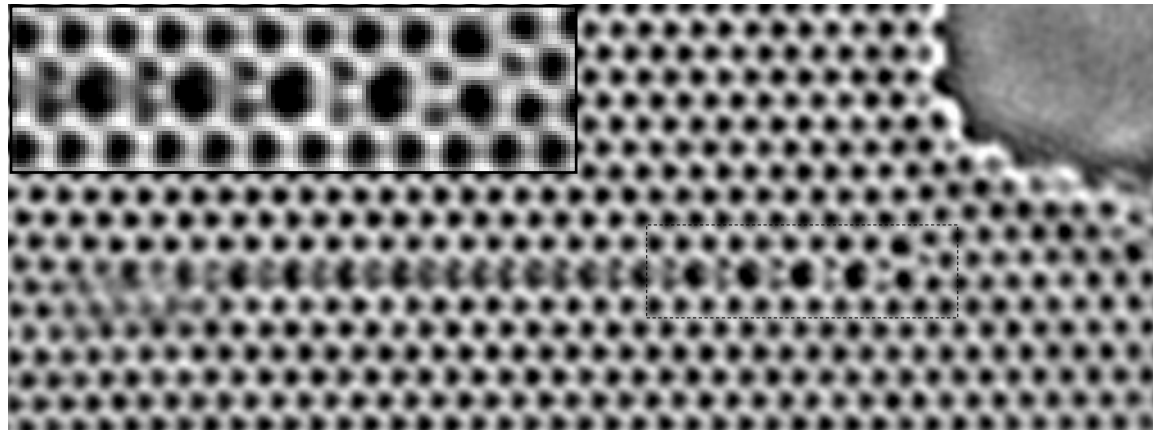
Why bother? **Valleytronics!**

Rycerz, Tworzydło & Beenakker, Nature Phys. **3**, 172 (2007)

# Controlled production of 5-5-8 line defect

Controlled production in TEM microscope + electric current:

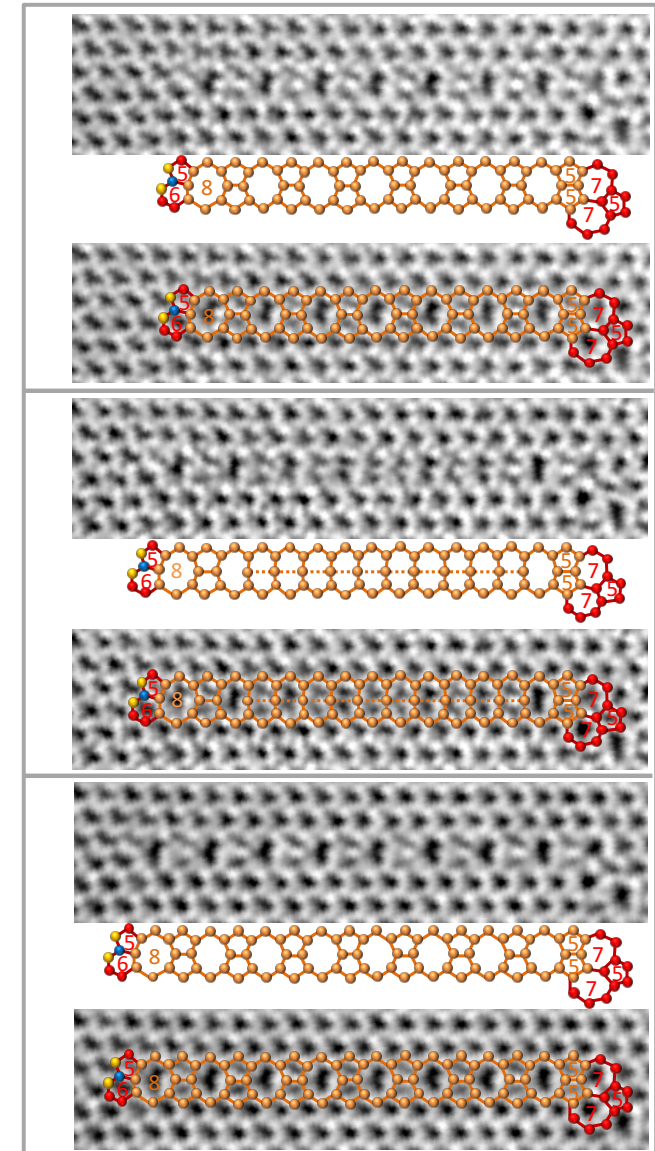
- Starts at the edge of a hole and proceeds via carbon atom removal;
- Combination of knock-on damage and electromigration (?)



mobile end  
 $E_{\text{term}} = 18 \text{ eV}$

pinned end  
 $E_{\text{term}} = 15 \text{ eV}$

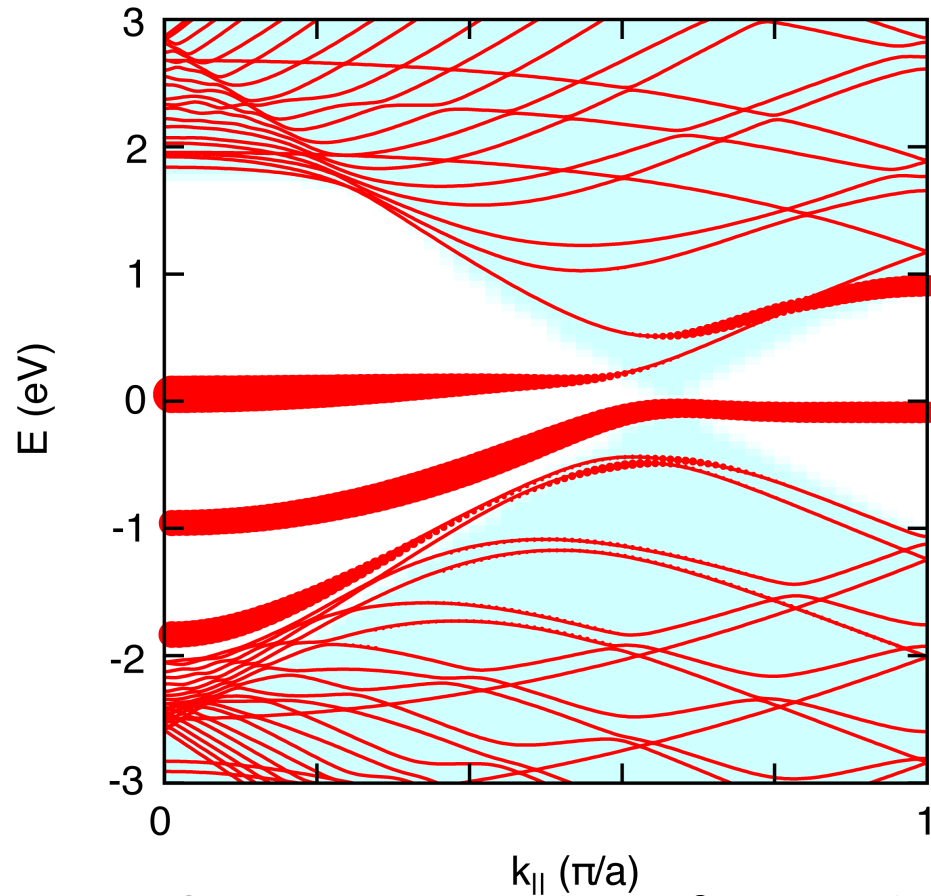
Growth dynamics:



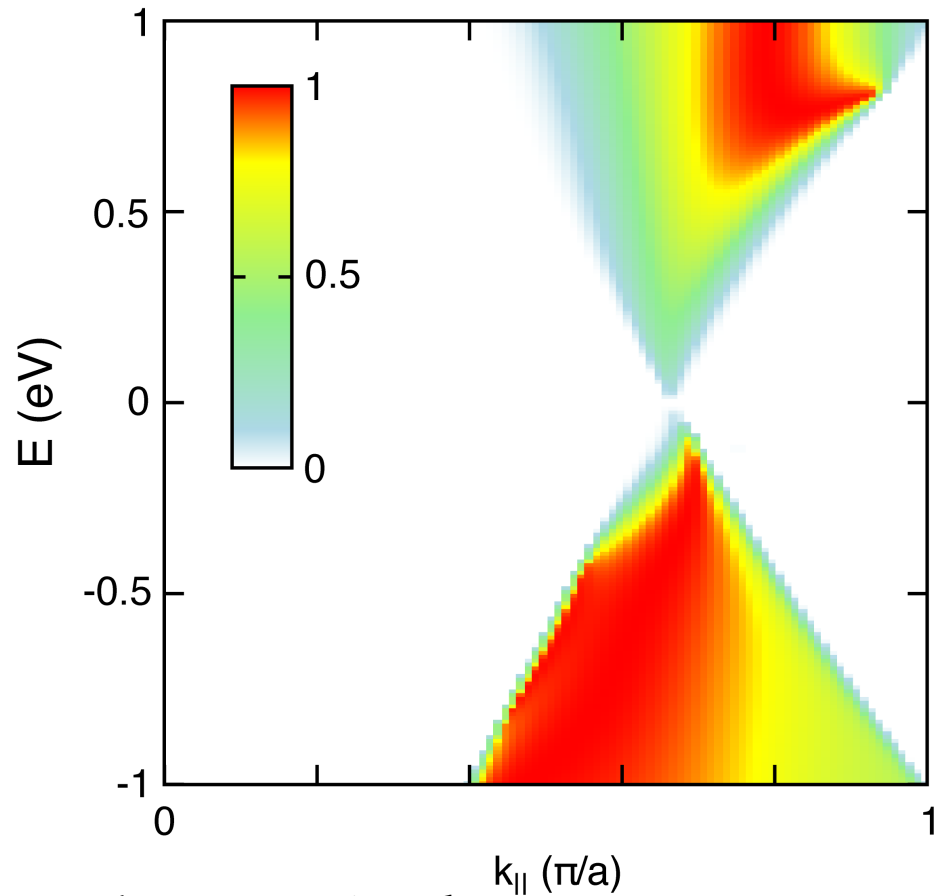
Experiments: Zettl group (UC Berkeley)

# First-principles results

band structure



transmission probability



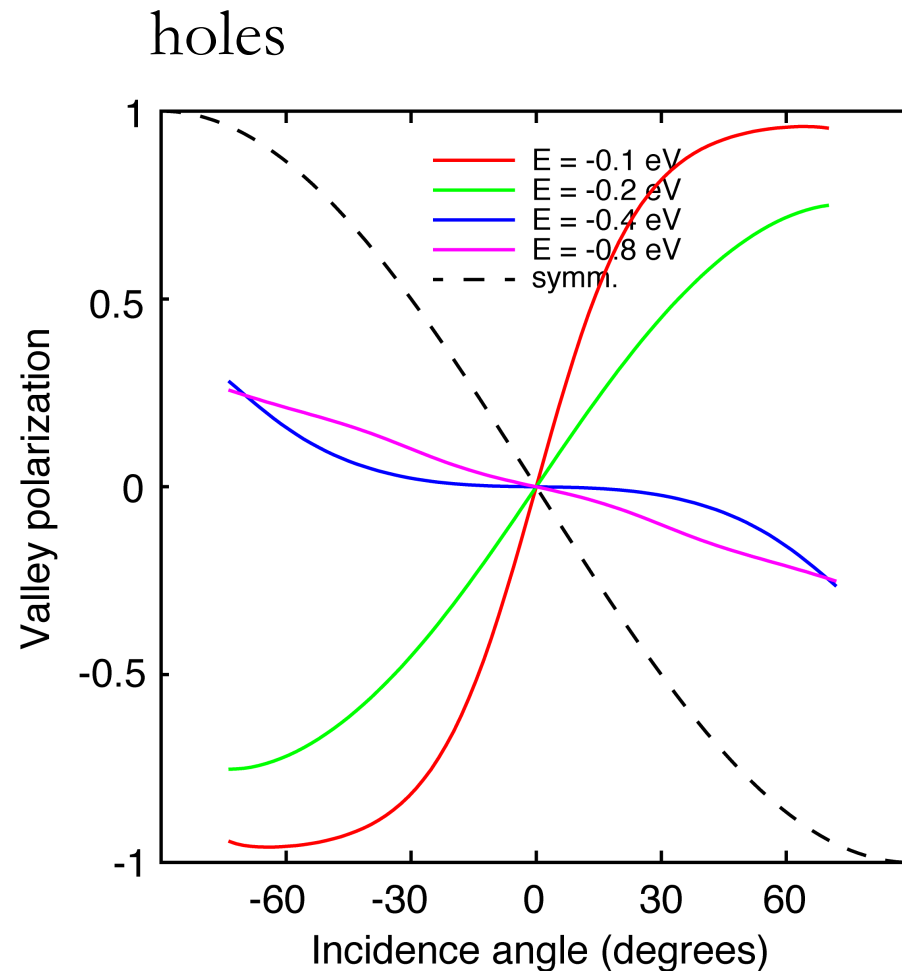
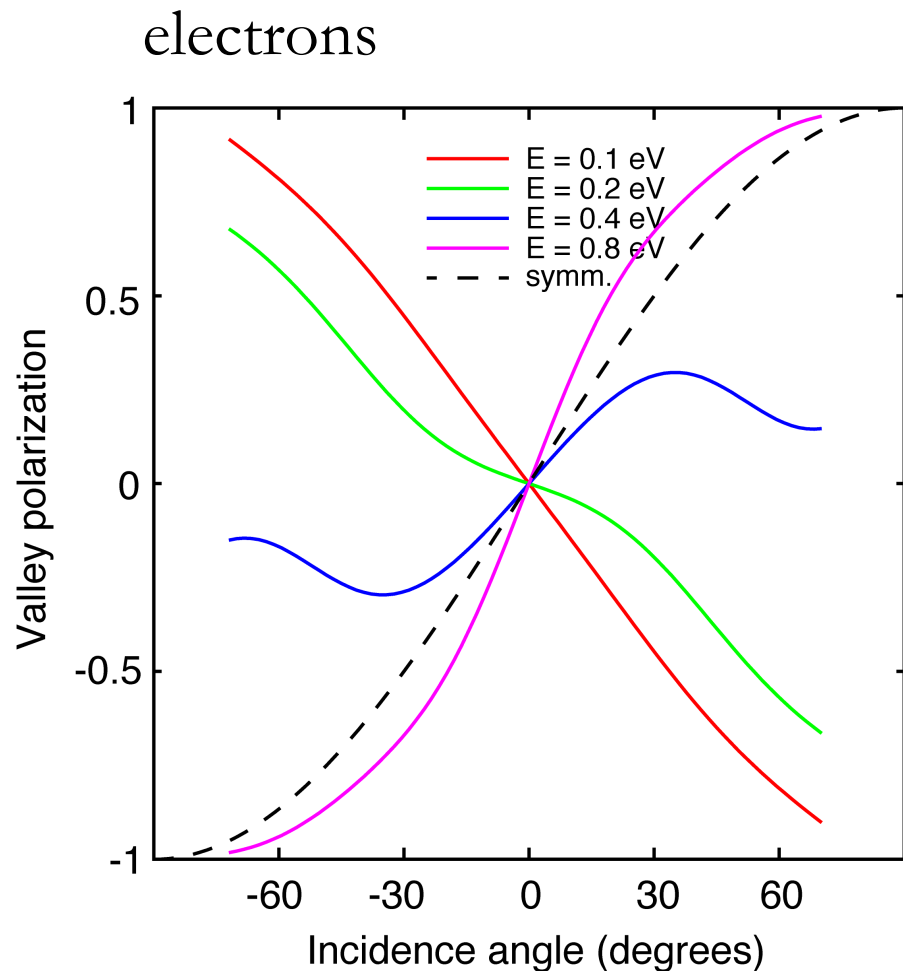
Strong suppression of transmission at low energies due to resonant backscattering on localized states

Calculations: Yazyev group (EPFL)

Chen *et al.*, Phys. Rev. B **89**, 121407 (2014)



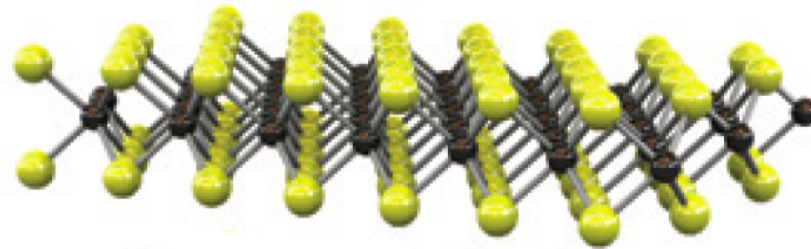
# Valley filtering from first-principles



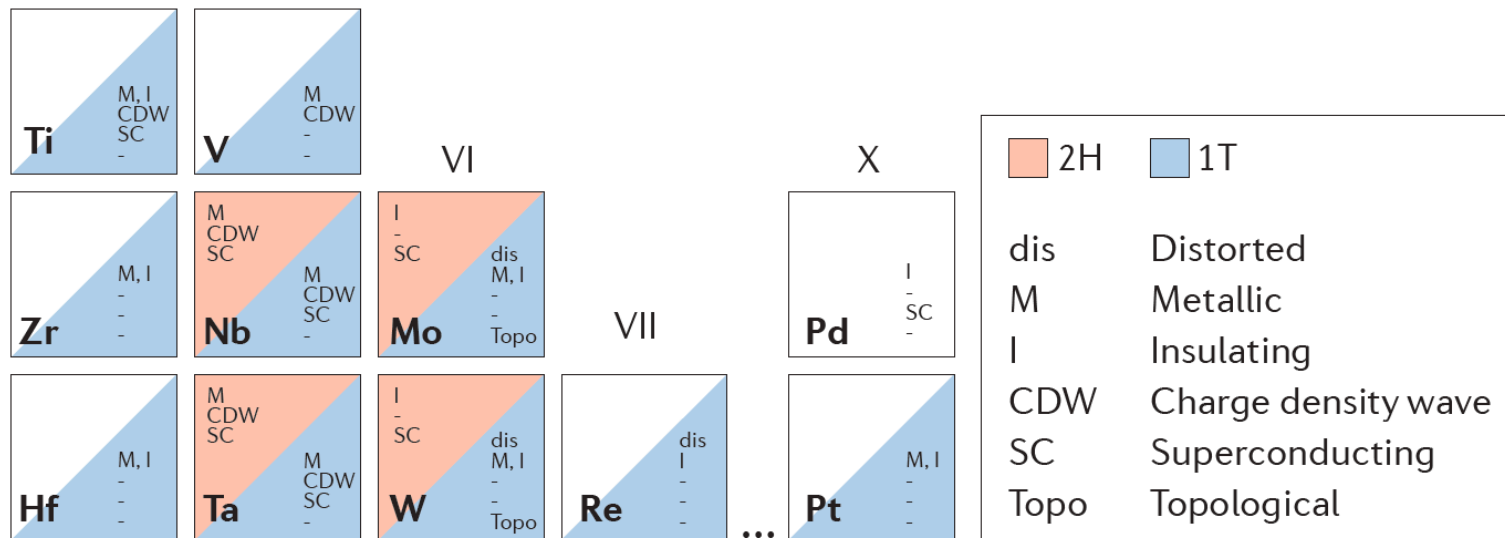
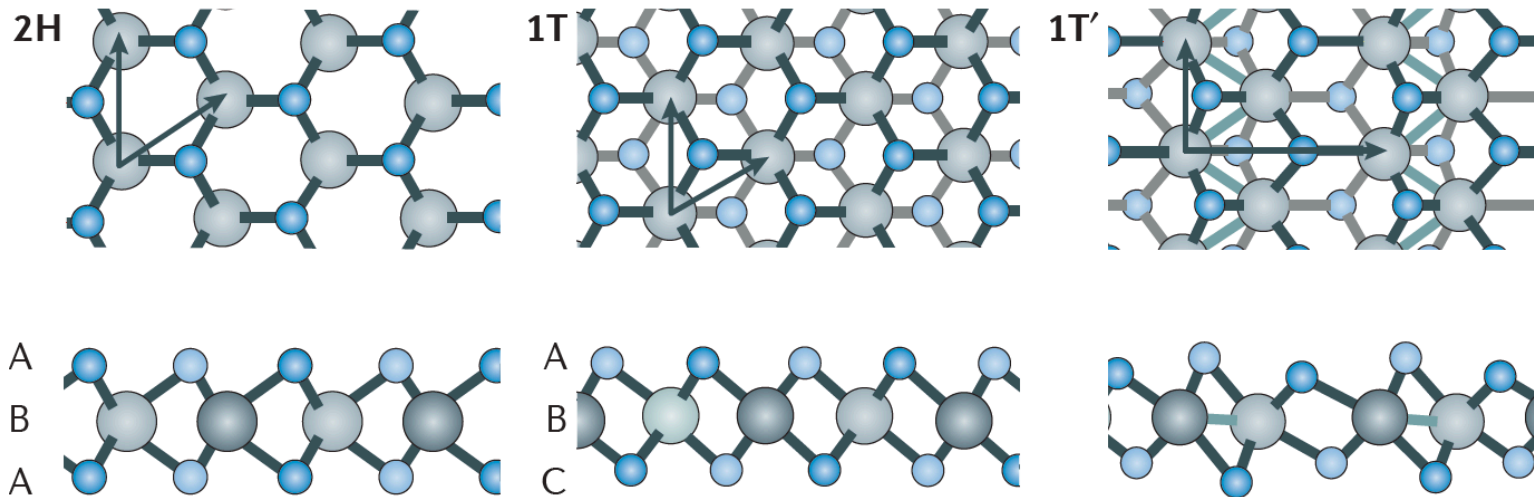
Strong energy dependence of valley polarization on charge-carrier energy

Calculations: Yazyev group (EPFL)  
Chen *et al.*, Phys. Rev. B **89**, 121407 (2014)

## IV. Valley/spin filtering in TMDs

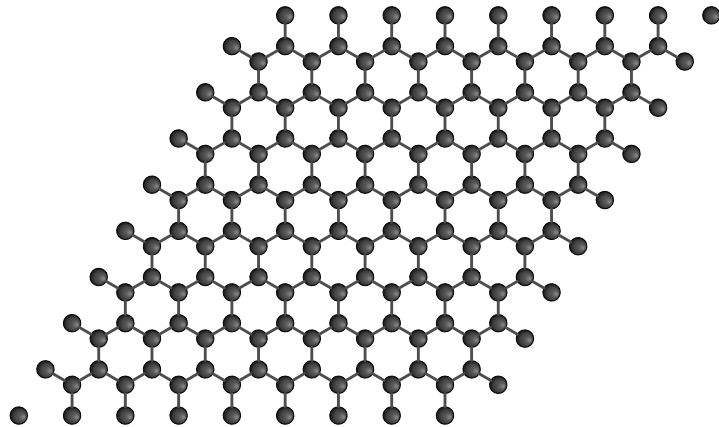
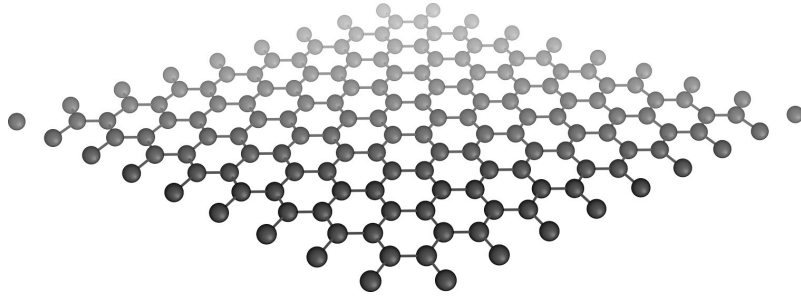


# 2D transition metal dichalcogenides (TMDs)



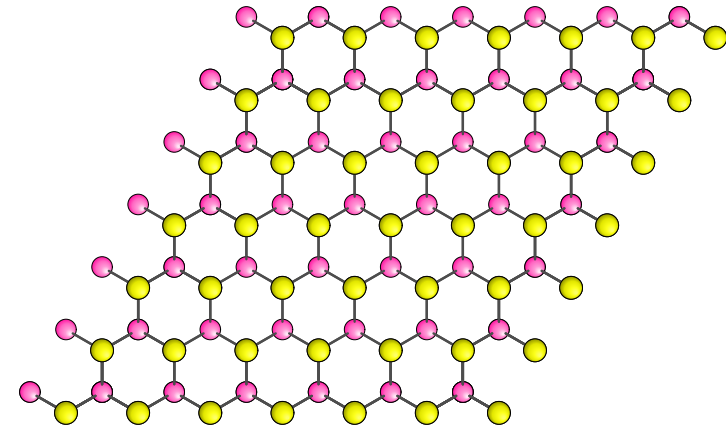
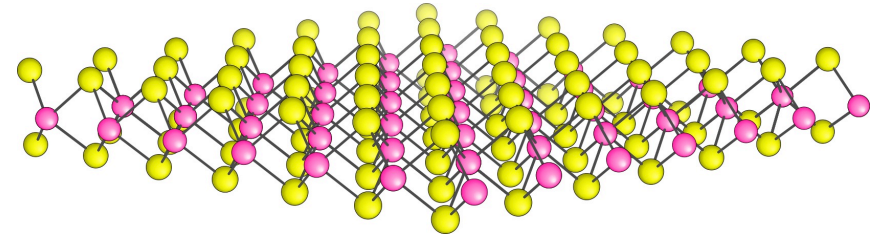
# Graphene vs. TMDs: atomic structure

graphene



- hexagonal symmetry
- equivalent sublattices
- centrosymmetric

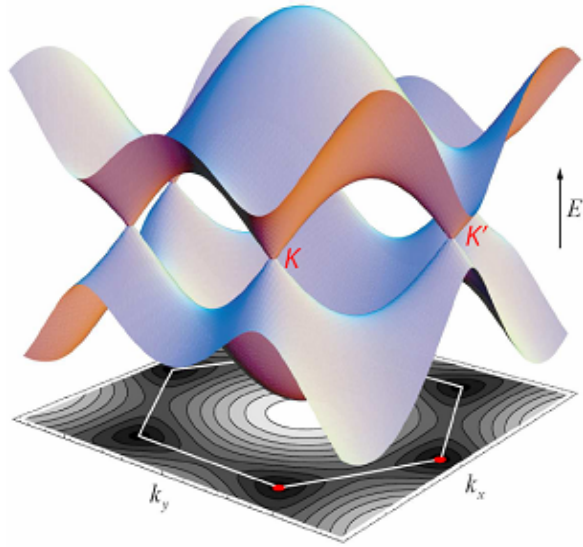
monolayer 2H MoS<sub>2</sub>



- hexagonal symmetry
- inequivalent “sublattices”
- non-centrosymmetric

# Graphene vs. TMDs: electronic structure

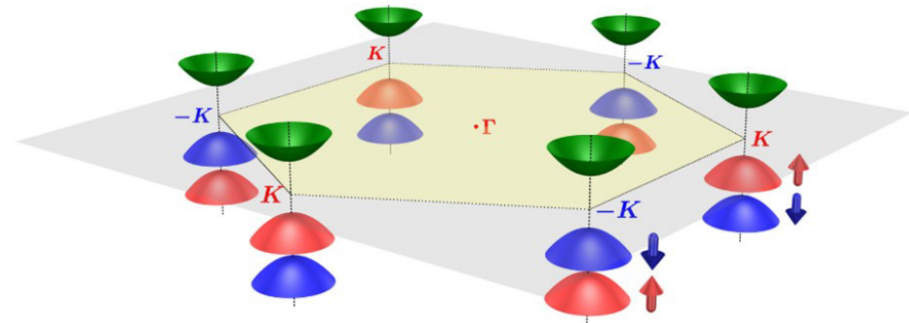
## graphene



- semi-metal ( $E_g = \sim 0$  eV)
- 2 valleys (points  $K$  and  $K'$ )
- very weak spin-orbit coupling ( $\Delta_{\text{SO}} = 2.4 \times 10^{-5}$  eV)

Gmitra *et al*, Phys. Rev. B **80**, 235431 (2009)

## monolayer 2H MoS<sub>2</sub>

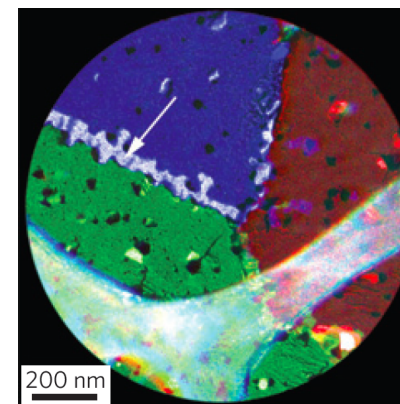
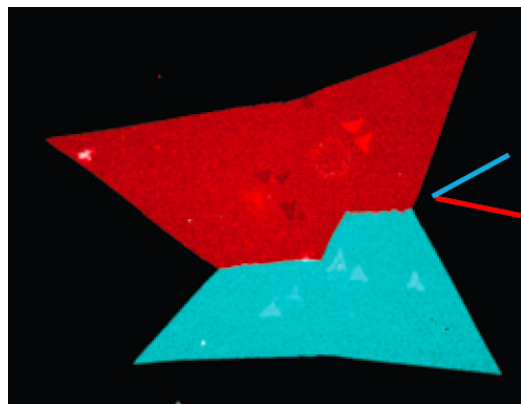


- semiconductor ( $E_g = 1.9$  eV, DFT)
- 2 valleys (points  $K$  and  $K'$ )
- strong spin-orbit coupling ( $\Delta_{\text{SO}} = 0.15$  eV for MoS<sub>2</sub>,  $\Delta_{\text{SO}} = 0.46$  eV for WSe<sub>2</sub>)

Zhu *et al*, Phys. Rev. B **84**, 153402 (2011)

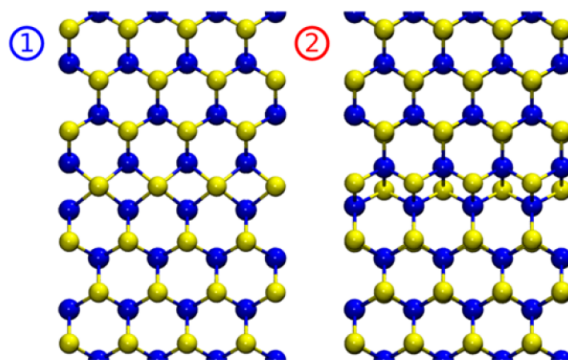
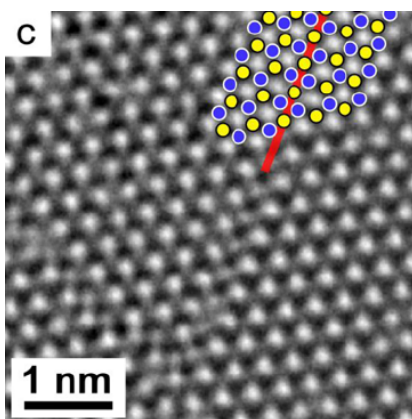
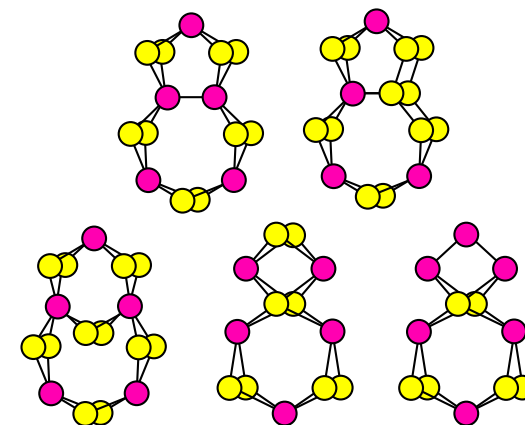
# Polycrystalline TMDCs

Aperture filtered DF-TEM images of CVD grown MoS<sub>2</sub>



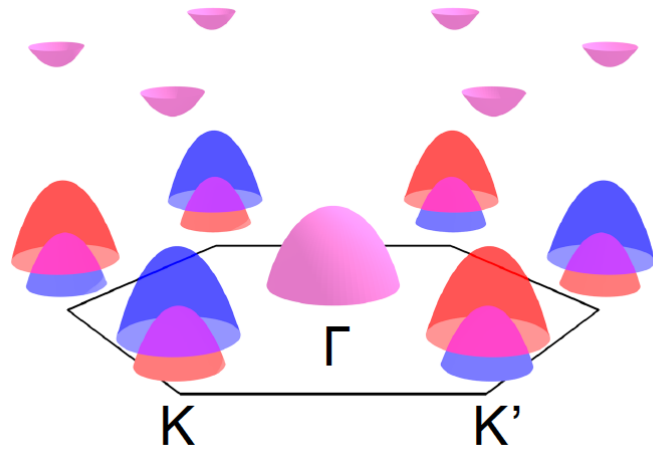
van der Zande *et al.*, Nature Mater. **12**, 554 (2013);  
Najmaei *et al.*, Nature Mater. **12**, 754 (2013).

- Highly faceted grain boundaries
- Many different structures possible
- Abundance of inversion domain boundaries

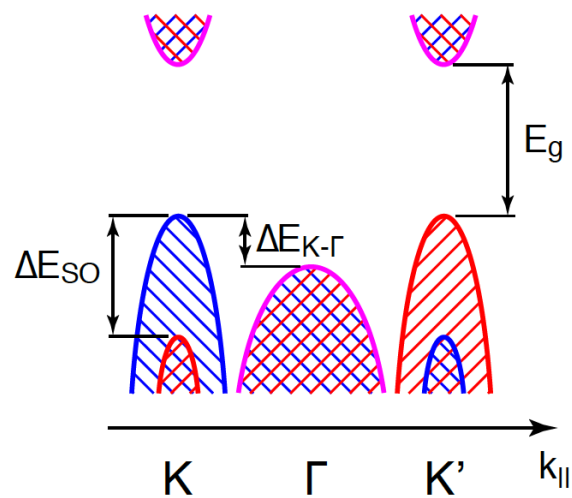


Zhou *et al.*, Nano Lett. **13**, 2615 (2013);  
Lin *et al.*, Nature Nanotech. **9**, 391 (2014)  
Lehtinen *et al.*, ACS Nano **9**, 3274 (2015).

# Possible transport scenarios

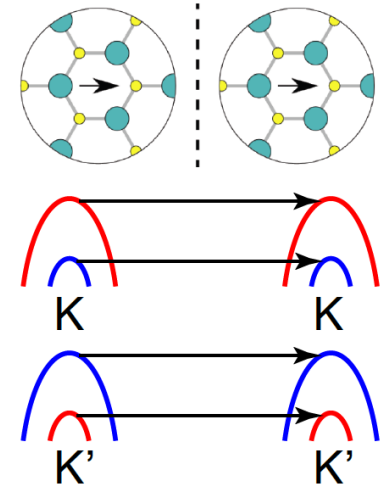


Band structure projected on lattice vector direction



Trivial scenario:

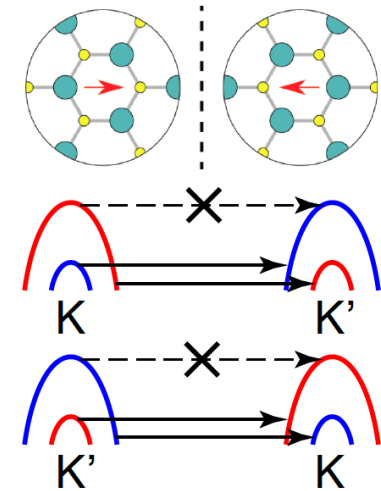
valley/*spin* filtering



Inversion domain boundary:

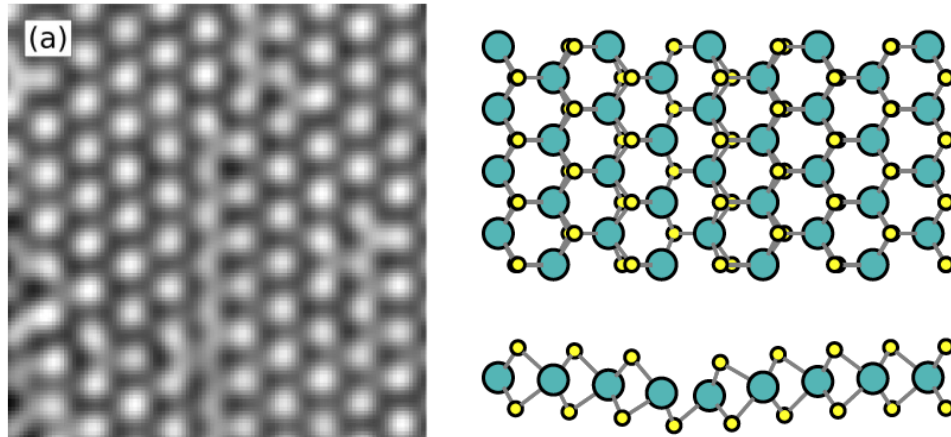
valley/*spin* filtering

+ transport gap



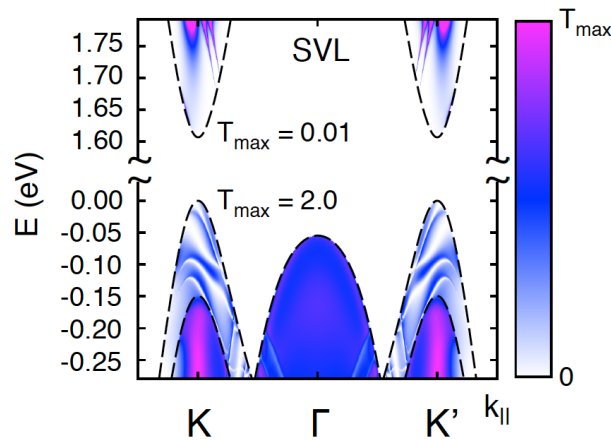
# Trivial scenario

Ordered sulfur vacancy lines

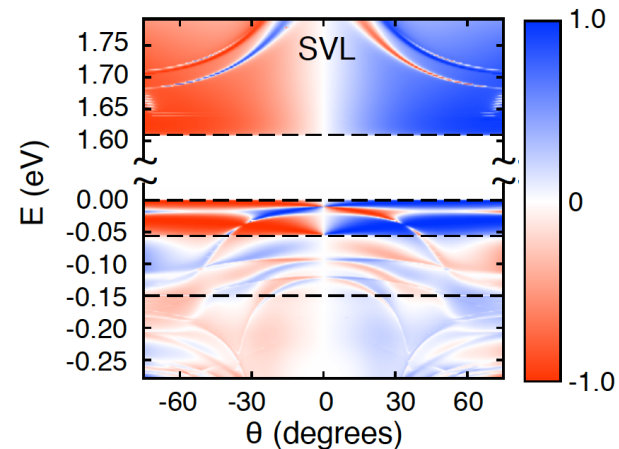


Komsa *et al.*, PRB **88**, 035301 (2013)

Transmission:



Valley/spin polarization:



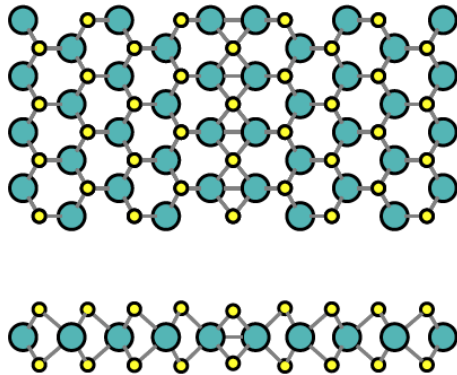
- nearly 100% spin polarization and large conductances of holes;
- contrasting transmissions asymmetry of electrons and holes

Pulkin & Yazyev, PRB **93**, 041419(R) (2016)

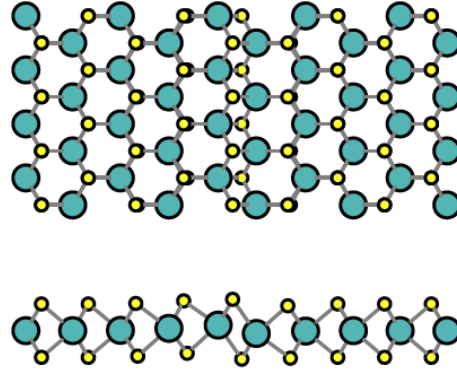


# Inversion domain boundaries

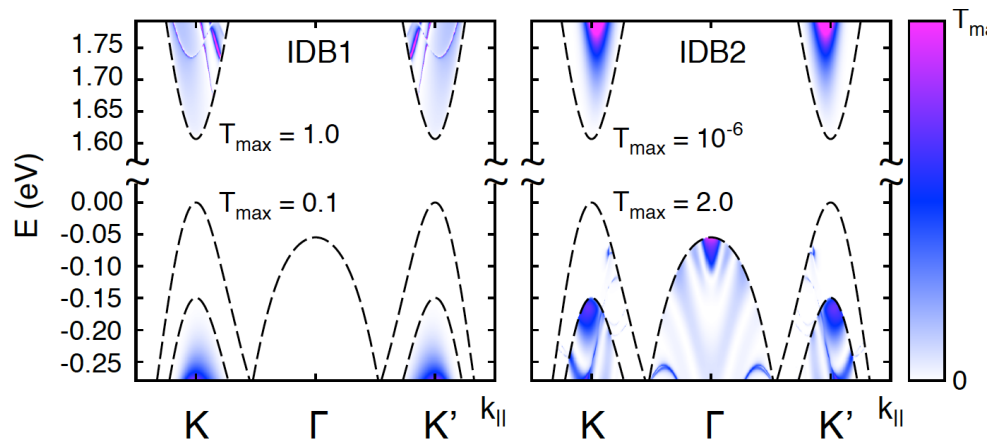
IDB1



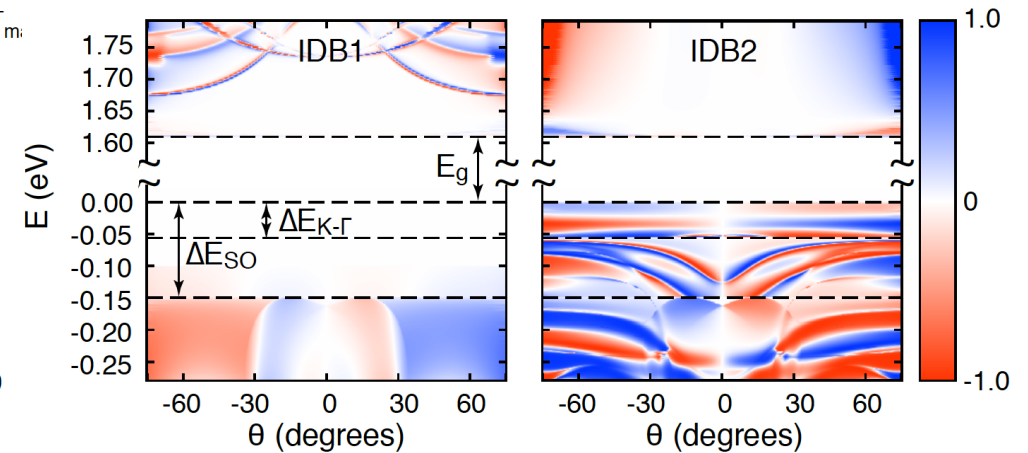
IDB2



Transmission:



Valley/spin polarization:



- spin-orbit transport gap of  $G$ - $K$  offset magnitude
- contrasting transmissions asymmetry of electrons and holes

# Acknowledgements

## My group



Fernando Gargiulo



Artem Pulkin



Gabriel Autès

and

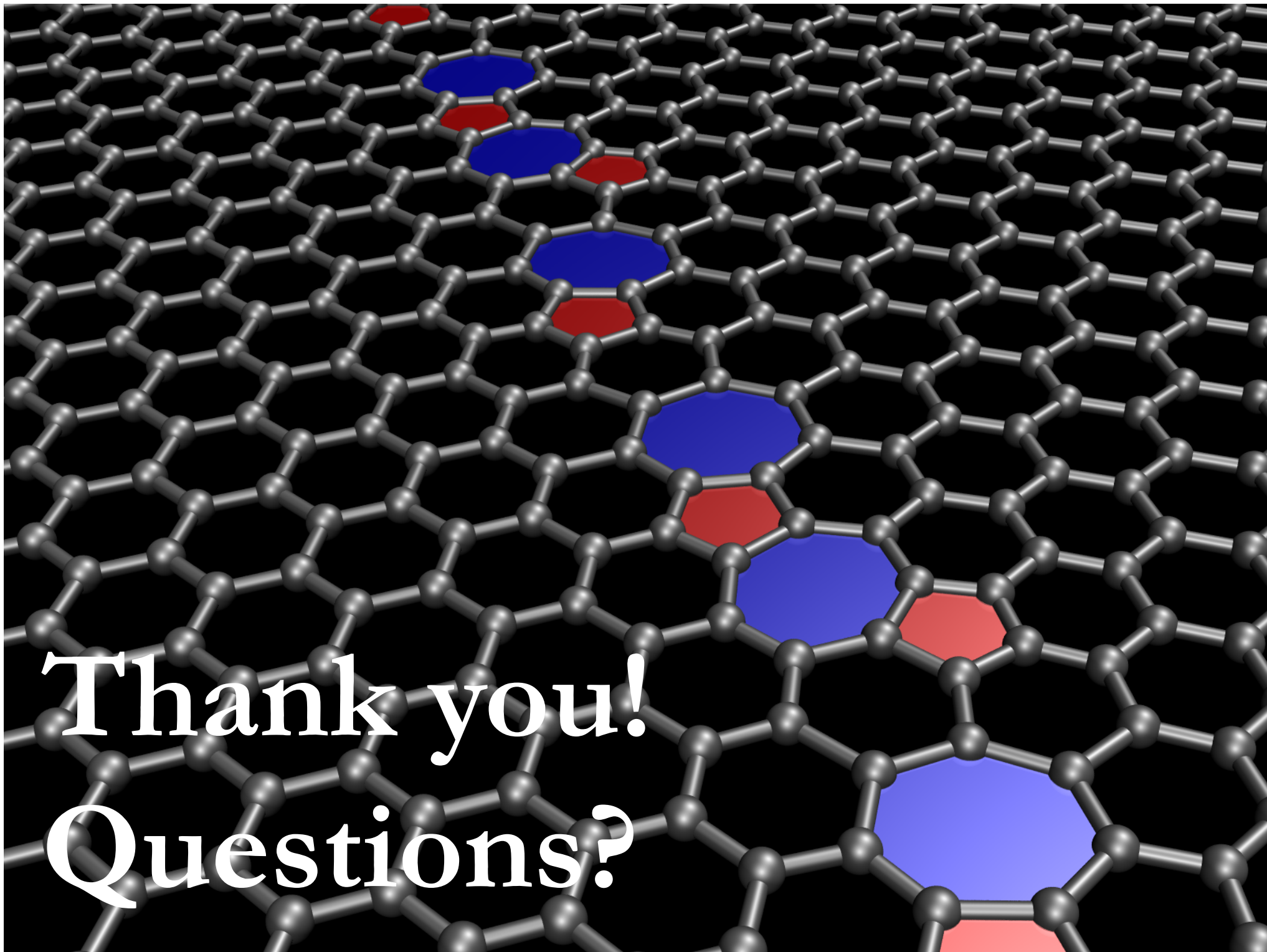
Steve Louie, Alex Zettl (UC Berkeley),  
Jérôme Lagoute, Vincent Repain (Paris VII),  
Andras Kis (EPFL), O. Lehtinen (Ulm)  
H.-P. Komsa, A. Krasheninnikov (Helsinki)

Funding:



European Research Council





Thank you!  
Questions?